Geophysical Journal International

Geophys. J. Int. (2014) **198,** 414–429
Advance Access publication 2014 May 21
GJI Seismology

doi: 10.1093/gji/ggu117

Upper mantle seismic anisotropy beneath the West Antarctic Rift System and surrounding region from shear wave splitting analysis

Natalie J. Accardo,[1,*] Douglas A. Wiens,[1] Stephen Hernandez,[2] Richard C. Aster,[3] Andrew Nyblade,[4] Audrey Huerta,[5] Sridhar Anandakrishnan,[4] Terry Wilson,[6] David S. Heeszel[7] and Ian W. D. Dalziel[8]

[1] *Department of Earth & Planetary Sciences, Washington University in St. Louis, St. Louis, MO 63130, USA. E-mail: accardo@ldeo.columbia.edu*
[2] *Department of Earth & Planetary Sciences, University of California, Santa Cruz, CA 95064, USA*
[3] *Geosciences Department, Colorado State University, Fort Collins, CO 80523, USA*
[4] *Department of Geosciences, The Pennsylvania State University, University Park, PA 16801, USA*
[5] *Department of Geological Sciences, Central Washington University, Ellensburg, WA 98926, USA*
[6] *Department of Geological Sciences, The Ohio State University, Columbus, OH 43210, USA*
[7] *Scripps Institution of Oceanography, University of California, San Diego, La Jolla, CA 92037, USA*
[8] *Institute for Geophysics, Jackson School of Geosciences, The University of Texas at Austin, Austin, TX 78712, USA*

Accepted 2014 March 25. Received 2014 March 15; in original form 2013 October 26

SUMMARY

We constrain azimuthal anisotropy in the West Antarctic upper mantle using shear wave splitting parameters obtained from teleseismic SKS, SKKS and PKS phases recorded at 37 broad-band seismometres deployed by the POLENET/ANET project. We use an eigenvalue technique to linearize the rotated and shifted shear wave horizontal particle motions and determine the fast direction and delay time for each arrival. High-quality measurements are stacked to determine the best fitting splitting parameters for each station. Overall, fast anisotropic directions are oriented at large angles to the direction of Antarctic absolute plate motion in both hotspot and no-net-rotation frameworks, showing that the anisotropy does not result from shear due to plate motion over the mantle. Further, the West Antarctic directions are substantially different from those of East Antarctica, indicating that anisotropy across the continent reflects multiple mantle regimes. We suggest that the observed anisotropy along the central Transantarctic Mountains (TAM) and adjacent West Antarctic Rift System (WARS), one of the largest zones of extended continental crust on Earth, results from asthenospheric mantle strain associated with the final pulse of western WARS extension in the late Miocene. Strong and consistent anisotropy throughout the WARS indicate fast axes subparallel to the inferred extension direction, a result unlike reports from the East African rift system and rifts within the Basin and Range, which show much greater variation. We contend that ductile shearing rather than magmatic intrusion may have been the controlling mechanism for accumulation and retention of such coherent, widespread anisotropic fabric. Splitting beneath the Marie Byrd Land Dome (MBL) is weaker than that observed elsewhere within the WARS, but shows a consistent fast direction, possibly representative of anisotropy that has been 'frozen-in' to remnant thicker lithosphere. Fast directions observed inland from the Amundsen Sea appear to be radial to the dome and may indicate radial horizontal mantle flow associated with an MBL plume head and low upper mantle velocities in this region, or alternatively to lithospheric features associated with the complex Cenozoic tectonics at the far-eastern end of the WARS.

Key words: Seismic anisotropy; Dynamics of lithosphere and mantle; Antarctica.

*Now at: Department of Earth and Environmental Sciences, Columbia University, New York, NY 10027, USA.

1 INTRODUCTION

Seismic anisotropy, the dependence of seismic velocities on propagation and polarization direction, has emerged as one of the best indicators of both past and present mantle deformation and flow (e.g. Silver & Chan 1988; Fischer *et al.* 1998; for a review see Long and Silver 2009). Mantle deformation often leads to seismic anisotropy; either through lattice preferred orientation (LPO) of anisotropic minerals or through shape preferred orientation (SPO) of materials having different seismic velocity. Because of the link between deformation and anisotropy, the mapping of anisotropic structure can yield some of the most direct constraints available on convection, deep tectonically induced deformation and generally on the coarse- and finer-scale fabric of Earth's mantle (Silver 1996; Savage 1999; Long & Becker 2010).

Olivine constitutes over 65 per cent of the upper mantle and, because it has a large single-crystal anisotropy (∼18 per cent; e.g. Mainprice *et al.* 2005), it is thought to make the primary contribution to the observed anisotropy. Laboratory studies of artificially deformed olivine aggregates indicate that multiple deformational fabrics (A-, B-, C-, D- and E-type) for olivine exist (for a review see Karato *et al.* 2008). The well-known A-type fabric promotes the alignment of the olivine fast axis with the direction of maximum shear, which may be in the extension and/or flow direction (Zhang & Karato 1995). Conversely, B-type fabric (favoured by high-stresses, low temperatures and the presence of water) predicts that fast axes will align normal to the direction of maximum shear (Jung & Karato 2001). Experimental studies have shown that the development of olivine fabrics depends greatly on the conditions of deformation, including, stress, water content, temperature and pressure (e.g. Katayama *et al.* 2004; Mainprice *et al.* 2005). There are multiple models that explain the presence of mantle seismic anisotropy, including: (1) mantle anisotropy induced by ongoing extension/compression due to the LPO of olivine, (2) anisotropy due to the alignment of parallel dikes or melt-filled lenses, (3) fossilized anisotropy in the lithospheric mantle due to LPO from past tectonic events. The detailed interpretation of anisotropic observations in terms of stress, strain, hydration, temperature and composition throughout the mantle is a complex and active area of research (e.g. Long & Silver 2009). Thus, while anisotropic fabrics are inherently complex, they provide unique information on the fabric of the mantle and hence on its deformational history and present state.

To date, very few seismic investigations have probed the mantle beneath Antarctica due to the harsh conditions of working there and the only recently resolved issues of maintaining seismographic stations there. Furthermore, no prior studies have examined the anisotropic nature of the West Antarctic Rift System (WARS), one of the largest regions of extended continental crust on Earth (Behrendt *et al.* 1991). Thus, determining the anisotropic character of the WARS has much to contribute to our understanding of mantle deformational fabrics associated with continental rifts, which are shown to vary significantly between different continental rift settings (e.g. Vinnik *et al.* 1992; Gao *et al.* 1997; Kendall *et al.* 2005; Obrebski *et al.* 2006; Wang *et al.* 2008; Eilon *et al.* 2014).

This study examines the seismic anisotropy beneath West Antarctica using shear wave splitting of SKS, SKKS and PKS phases obtained from 37 broad-band seismometres deployed in the WARS and throughout the rest of West Antarctica, including Marie Byrd Land (MBL) and in the Transantarctic Mountains (TAM). These data allow us to better understand the deformational history and mantle flow patterns of a largely unexplored continental region where geologic exposures occupy less than 2 per cent of the surface area. Inferences on mantle flow processes beneath West Antarctica provides unique constraints on the deformational history of the geology that underlies and strongly influences the West Antarctic Ice Sheet (e.g. Winberry & Anandakrishnan 2004; Bingham *et al.* 2012).

2 GEOLOGIC SETTING

Antarctica is naturally divided into two distinct major provinces: East Antarctica and West Antarctica. East Antarctica is comprised of a large stable continental craton composed mainly of Precambrian basement rocks that are uncomformably overlain by sedimentary units. In contrast, West Antarctica comprises a number of discrete mountainous crustal blocks that moved relative to East Antarctica and each other during broad extension dating back to the Jurassic (Dalziel & Elliot 1982; Dalziel 1992; Anderson 1999). They were derived from the margin of the East Antarctic craton and from the Pacific convergent margin. The TAM, the largest non-compressional mountain belt in the world, separates the two provinces (e.g. ten Brink *et al.* 1997).

2.1 The Transantarctic Mountains

The TAM are a gently tilted to block-faulted mountain range characterized by an absence of folding or thrust faulting. They extend for over 3500 km from the Ross Sea to the Weddell Sea, prominently separating the Ross Embayment, a vast submerged region of extended continental crust that is partially covered by Earth's largest ice shelf, from the icecap-covered Wilkes subglacial basin (ten Brink *et al.* 1997). The TAM owes its earliest origins to the Neoproterozoic Beardmore Orogen and was later intensely deformed by the early Paleozoic Ross Orogeny (Borg *et al.* 1990). The exact timing of the uplift(s) of the present TAM remains poorly constrained. Apatite fission track thermochronology from Victoria Land and the South Pole indicates that separate blocks of the TAM have experienced varying amounts of uplift and erosion at different times, ranging from Early Cretaceous to Cenozoic (Fitzgerald 1992, 1994; Stump & Fitzgerald 1992; Balestrieri *et al.* 1994). The relationship between the formation of the TAM and the WARS remains unclear despite their obvious spatial relationship (Fig. 1). Major WARS extension during the Cretaceous was apparently accompanied by relatively little denudation in the TAM, whereas limited extension during the Cenozoic was accompanied by large amounts of denudation (Karner *et al.* 2005; Huerta & Harry 2007). Geodynamic models of the WARS evolution suggest that the TAM may be the abandoned margin of a Mesozoic West Antarctic plateau, and the Cretaceous through Cenozoic crustal cooling ages of the TAM record initial subsidence of the WARS region followed by fluvial and glacial denudation of the mountain range (Bialas *et al.* 2007; Huerta & Harry 2007).

2.2 The West Antarctic Rift System

The WARS abuts the TAM and is generally characterized by a topographic trough 750–1000 km wide and 3000 km long (e.g. Behrendt *et al.* 1991). It is often described as an asymmetric rift system that is proposed to run from the Ellsworth-Whitmore mountains crustal block (EWM) to the edge of the Ross Embayment where it meets northern Victoria Land (Fig. 1). The region is characterized by a regional positive Bouguer gravity anomaly that extends from the Ross Sea throughout the Byrd Subglacial Basin (Behrendt & Cooper 1994). Uncertainty still persists on the timing and evolution of the

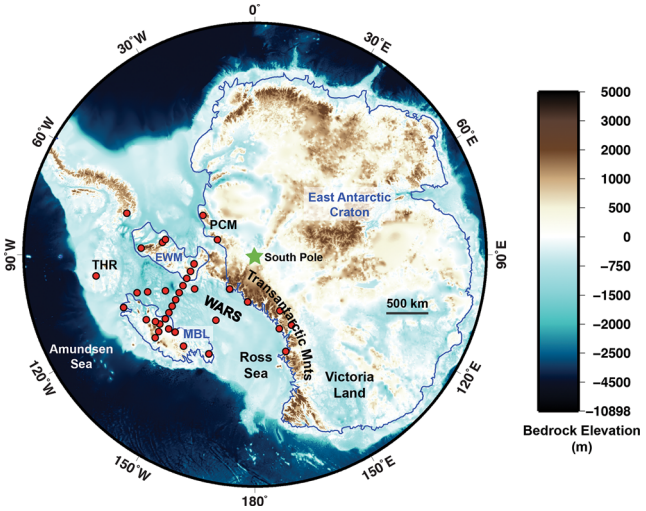

Figure 1. POLENET/ANET station locations (red circles) used in this study and geologic regions of interest; WARS, West Antarctic Rift System; EWM, Ellsworth-Whitmore Mountains crustal block; PCM, Pensacola Mountains; MBL, Marie Byrd Land; THR, Thurston Island crustal block. The boundaries for the East Antarctic Craton, the EWM crustal block, and the MBL crustal block from Dalziel & Elliot (1982) are drawn in blue. Background colour scale shows bed elevation beneath the ice sheets (Fretwell *et al.* 2013). Black bar indicates the scale of 500 km.

WARS because of extensive ice cover and limited number of geological and geophysical studies conducted in this region. The total extension accommodated by the WARS crust is poorly constrained, and estimates vary widely. Busetti *et al.* (1999) estimate 120–250 km, Grindley & Oliver (1983) estimate 200–500 km, numerous authors (e.g. Fitzgerald *et al.* 1986; Behrendt & Cooper 1994) estimate 255–300 and Trey *et al.* (1999) estimate 480–500 km. Recent studies show that portions of the WARS are underlain by extremely thin continental crust, as thin as ∼20 km near the Bentley Trench, in the vicinity of Ross Island and the Byrd Basin (Winberry & Anandakrishnan 2004; Chaput *et al.* 2014), indicating significant localized crustal thinning separating the East Antarctic craton and the EWM crustal block from the MBL and Thurston Island crustal blocks.

Studies suggest extension has occurred in two major pulses, with the first during the Jurassic-Cretaceous, inducing major distributed crustal thinning over the entire WARS. A second pulse later in the Cenozoic is widely documented in the Ross Sea region (e.g. Behrendt 1999; Karner *et al.* 2005; Wilson & Luyendyk 2006). Cenozoic extension may thus have itself occurred in two stages, with an earlier period from 41 to 26 Ma concentrated in the Ross Sea region and a Miocene pulse affecting mostly regions further inland (Granot *et al.* 2010; Granot *et al.* 2013). Whether or not the rifting occurred in several pulses, it is generally accepted that the major extension of the region commenced ca. 105 Ma (Luyendyk 1995; Siddoway *et al.* 2004) and slowed by ca. 17 Ma (Cande *et al.* 2000; Hamilton *et al.* 2001; Granot *et al.* 2010). Presently, the low level of seismicity (Winberry & Anandakrishnan 2004) and GPS measurements indicating low strain rates between East and West Antarctica (e.g. Donnellan & Luyendyk 2004; Wilson *et al.* 2011) suggest that the rift is currently inactive or extending very slowly.

The WARS differs from other continental rifts in several important respects. The diffuse Jurassic-Cretaceous extension of the WARS affected a much wider region relative to most continental rifts (Huerta & Harry 2007), such as the Baikal Rift, East African Rift and North American Midcontinent Rift (Logatchev *et al.* 1983; Ingersoll *et al.* 1990; Keller *et al.* 1991). Also the extremely deep WARS rift floors are at much lower elevations than other continental rift zones, even when deglaciated and rebound is considered (LeMasurier 2008). The WARS crust is generally thin, with aforementioned areas of very thin crust beneath much of the West Antarctic Ice Sheet, increasing to a maximum near 30 km in western MBL (Chaput *et al.* 2014). Comparisons of rift floor elevations in conjunction with the unique extensional history of the WARS show that the system does not conform to the behaviour expected from previously investigated continental rifts or broad regions of extension like the U.S. Basin and Range.

Cenozoic bimodal alkali volcanic rocks, commonly found within continental rifts, characterize the MBL shoulder of the WARS (e.g. LeMasurier 1990), and aeromagnetic surveys suggest the presence of these rocks over an area of $>5 \times 10^5$ km^2 within the rift itself. The absence of abundant exposures makes it difficult to estimate when the bulk of late Cenozoic volcanic rocks erupted. Nevertheless, available radiometric ages extend from the present back to 30 Ma (LeMasurier 1990). An active mantle plume (Behrendt *et al.* 1991), intraplate tectonic displacements induced by the plate circuit of the Southern Hemisphere (Rocchi *et al.* 2002), and thermal perturbation of metasomatized lithosphere (Finn *et al.* 2005) have all been proposed as mechanisms of magma generation and emplacement, although these hypotheses remain largely untested.

The extent of the WARS towards the Antarctic Peninsula remains conjectural, as most geophysical campaigns to date have concentrated on the more accessible and better geologically exposed Ross Sea region (e.g. Behrendt *et al.* 1996; Trey *et al.* 1999; Karner *et al.* 2005). However, it seems likely from ice rebound-adjusted topography (e.g. Chaput *et al.* 2014) that the WARS extensional zone continues to the Pacific coast in the Amundsen Sea region. Subglacial basins in the Bentley Trench/Amundsen Sea region are comparable in lateral extent to those within the Ross Sea, yet reach much greater surface depths. The deepest portions of these basins extend more than 1500 m below sea level, making them the lowest elevation continental topographic features on Earth. These basins and troughs likely accommodated lateral motion during the Eocene-Oligocene when the region underwent a period of significant convergence (Granot *et al.* 2013). Recent aeromagnetic and aerogravity surveys have identified rifts in the Pine Island and Ferrigno areas, both locations of gravity and magnetic anomalies consistent with other recently active rifts, that are mechanically related to the central WARS (Jordan *et al.* 2010; Bingham *et al.* 2012). These features show evidence for only small amounts of sediment infill, suggesting that they may have only opened during the last pulse of WARS extension in the Neogene (Bingham *et al.* 2012).

2.3 The Ellsworth-Whitmore Mountains crustal block and Pensacola Mountains

The EWM, located at the head of the Weddell Sea embayment, represent a geologically and geophysically distinct crustal block within West Antarctica (Dalziel & Elliot 1982). The EWM are anomalous in stratigraphy, structural grain and deformational history relative to their surroundings. Geologic and palaeomagnetic investigations strongly indicate that the EWM underwent extensive translation and rotation from their initial location prior to the breakup of Gondwana (e.g. Clarkson & Brook 1977; Watts & Bramall 1981; Curtis 2001; Randall & Niocaill 2004). The stratigraphy of the EWM does not correlate with that of any other part of West Antarctica but instead exhibits obvious ties to the Gondwana craton margin sequences seen

within the TAM (Schopf 1969). The structural trend of the EWM strikes close to transverse to both the TAM and, in a reconstructed Gondwana supercontinent, the Cape Fold Belt in Africa. Beginning in the 1960s, numerous authors have suggested that these enigmas can be resolved if the EWM originated at a location adjacent to the palaeo-Pacific margin of Gondwana, between South Africa and the Coats Land coast of Antarctica, and later underwent lateral translation and rotation along the Antarctic margin during Gondwana breakup (e.g. Schopf 1969; Dalziel 1992; Goldstrand *et al.* 1994). More recent palaeomagnetic and stratigraphic investigations have largely confirmed that the EWM previously sat adjacent to South Africa in a proposed continental rift basin prior to Gondwana breakup (Curtis 2001; Randall & Niocaill 2004). The EWM crustal block composes thicker crust and seismically faster upper mantle than the surrounding WARS (Heeszel *et al.* 2011; Lloyd *et al.* 2012; Chaput *et al.* 2014), consistent with the idea that it is indeed a fragment of older pre-extensional continental lithosphere.

The Pensacola Mountains (PCM) lie between the northern TAM termination and the Weddell Sea margin (Fig. 1). The PCM show many geologic features common along the TAM, such as late Neoproterozoic to Late Paleozoic magmatic and sedimentary sequences deformed during a series of Neoproterozoic to early Paleozoic orogenic events related to the end of the Ross Orogeny (Stump 1995; Rowell *et al.* 2001). In a large-scale sense, the PCM are a continuation of the TAM, also representing an extensional uplift of the older orogeny formed along the edge of the East Antarctic Craton.

2.4 The Marie Byrd Land Dome

The MBL intraplate volcanic province is a large region defined by a 1000 × 550 km dome that broadly rises to approximately 2000 m in deglaciated surface elevation and is punctuated by volcanoes reaching deglaciated elevations over 4000 m. The main MBL dome is approximately centred on a belt of mid-to-late Cenozoic alkaline volcanoes that extends along Antarctica's Pacific Coast. The MBL province is one of two regions within this belt where large central vent volcanoes with more than 2000 m of relief are found (LeMasurier & Rex 1989). The WARS lies polewards of MBL and separates it from the TAM and the EWM. Crustal thicknesses (26–28 km) beneath the volcanic province are 2–5 km greater than they are within much of the WARS (Chaput *et al.* 2014). Thinner crust is also found to the east of MBL in the region of Pine Island Glacier (Jordan *et al.* 2010; Chaput *et al.* 2014).

Lines of volcanoes divided by subglacial basins characterize the landscape within the MBL dome (LeMasurier & Rex 1989). The Cenozoic volcanic deposits of the MBL overlie mid- and pre-Cretaceous rocks. The exposed Jurassic and Lower Cretaceous rocks in the MBL dome region are mostly igneous I-type granites and related volcanic rocks, while the mid-Cretaceous rocks are A-type granitoids thought to have formed at mid-crustal levels and then exposed during extension before the breakup of Gondwana in this region. These formations are thought to reflect a transition between subduction- to rift-related magmatism prior to the separation of the New Zealand microcontinent (Weaver *et al.* 1994). Volcanic activity continued in the Holocene (i.e. Dunbar *et al.* 2008) and recent studies have identified deep earthquakes polewards of Mount Sidley and Mount Waesche, indicating that the region remains magmatically active today (Lough *et al.* 2013).

Prior to Gondwana breakup, MBL sat between East Antarctica and New Zealand, where the Phoenix Plate was subducting. The separation of New Zealand from the Antarctic core of Gondwana in the Late Cretaceous was the last in a series of fragmentation events during the breakup of the supercontinent (Storey 1995). Granites from the Ruppert and Hobbs coasts of MBL indicate a prolonged period of subduction-related magmatism beginning at 320 ± 3 Ma or earlier (Mukasa & Dalziel 2000). Subduction ceased at ca. 108 Ma as a result of either collision of the Pacific-Phoenix spreading ridge with the subduction zone (Bradshaw 1989) or abandonment of the spreading ridge by slab capture (Luyendyk 1995). After subduction stopped, plate boundary forces changed dramatically and separation accelerated. Evidence for ocean floor development between New Zealand and MBL by 81 Ma suggests that complete separation of the continental blocks had occurred by that time (Mukasa & Dalziel 2000).

Many authors have proposed the existence of a mantle plume beneath MBL beginning in the Cenozoic (LeMasurier & Rex 1989; Behrendt *et al.* 1991; Hole & LeMasurier 1994; Sieminski *et al.* 2003) to account for the intraplate MBL Cenozoic alkaline basaltic province. It has also been suggested that a mantle plume might have existed beneath MBL beginning in the mid-Cretaceous and coincident with initial WARS opening (Storey *et al.* 1999) but this earlier plume hypothesis is more controversial. Mantle plumes have been linked to lithospheric extension in both the East African rift (e.g. Schilling 1973a; Ritsema *et al.* 1999) and the Reykjanes Ridge (e.g. Schilling 1973b; Gaherty 2001) and thus could be expected to potentially play a role within the WARS. High heat flow measurements in the Ross Sea (66–114 mW m^{-2}; Blackman *et al.* 1987) and at the West Antarctic Ice Sheet drill site (240 mW m^{-2}; Clow & Cuffey 2012), limited Cenozoic extension that, to first order, seems unable to account for the volume of observed volcanism, and geochemical similarity between the MBL basalts and oceanic island basalts can be taken to be supportive of the plume hypothesis (LeMasurier & Rex 1989; Hole & LeMasurier 1994).

3 DATA AND METHODS

3.1 Data

Data from 37 broad-band seismic stations installed throughout West Antarctica between 2007 and 2011 as part of the POLENET/ANET project are examined here. Table 1 gives station names and locations. Many of the stations form a part of the POLENET/ANET backbone array, and most are co-located with GPS sensors near nunataks and larger rock outcrops. A number of temporary stations deployed for 2 yr (station names beginning with ST and hereafter referred to as the POLENET transect) operated for a shorter time than backbone stations in a line extending from the Whitmore Mountains, through the WARS, and across the MBL dome. Fig. 1 shows station locations as well as prominent geologic and geographic features within West Antarctica. Reliable year-round station operation was accomplished using a combination of lead-acid batteries, specially insulated enclosures, and winter-use primary lithium batteries designed and supported by the IRIS PASSCAL program (Nyblade *et al.* 2012).

Earthquake sources used for this study were selected for USGS NEIC-determined $M_w > 6.0$ and epicentral distances between 90° and 140°. SKS, SKKS and PKS phases were carefully examined, and only those with a sufficient signal-to-noise ratio (SNR) and that were clearly separated from other phases were chosen for analysis. The highest SNR seismograms were analysed without filtering; these were generally evaluated as the highest quality results. Records with lower SNR were bandpass filtered with a low frequency corner of 0.02 Hz and a variable high frequency corner between 0.15 and 0.5 Hz.

Table 1. Summary of anisotropic parameters determined in this study. Grid fast direction indicates the fast direction relative to a rectangular Grid stereographic convention where north is taken to be along the prime meridian, south becomes the 180° meridian, east becomes 90°E, and west becomes 270°E. Values in parentheses under the 'Phases Used' column indicate the number of null observations reported for each station. Null observations were not utilized when stacking for the final splitting parameters.

Station	Latitude	Longitude	Geographic fast direction (degree)	Phi standard error (+/−)	Grid fast direction (degree)	Splitting time (s)	Splitting time standard error (+/−)	Phases used	Grade
BEAR	−74.548	−111.851	61	5	−51	0.75	0.1125	4 (2)	B
BYRD	−80.017	−119.473	−38	2	22	0.68	0.0625	5 (3)	B
CLRK	−77.323	−141.849	7	13	45	0.70	0.275	3 (0)	B
DEVL	−81.476	161.975	25	15	6	0.60	0.25	2 (2)	B
DNTW	−76.457	−107.780	−84	1	−12	0.60	0.0375	5 (3)	B
DUFK	−82.862	−53.201	−42	0	84	0.95	0.0375	20 (2)	A
FALL	−85.307	−143.628	−2	2	34	0.50	0.0375	8 (2)	A
FISH	−78.928	162.565	53	15	35	0.40	0.1125	4 (2)	B
HOWD	−77.529	−86.769	−65	4	28	0.55	0.05	9 (2)	A
KOLR	−76.155	−120.728	–	–	–	–	–	–	C
LONW	−81.347	152.735	−75	5	77	0.60	0.0625	4 (0)	B
MECK	−75.281	−72.185	–	–	–	–	–	–	C
MILR	−83.306	156.252	–	–	–	–	–	–	C
MPAT	−78.030	−155.022	21	7	45	0.45	0.0625	4 (1)	B
PECA	−85.612	−68.553	−70	1	41	0.90	0.0375	10 (0)	A
SILY	−77.133	−125.966	−42	3	12	0.55	0.0375	11 (0)	A
SIPL	−81.641	−148.956	−18	1	13	0.73	0.0375	15 (3)	A
ST01	−83.228	−98.742	−72	3	9	1.15	0.0375	7 (3)	A
ST02	−82.069	−109.124	−42	2	28	1.30	0.04	12 (2)	A
ST03	−81.407	−113.150	−37	0	29	1.28	0.025	11 (3)	A
ST04	−80.715	−116.578	−38	1	25	1.43	0.075	5 (1)	A
ST06	−79.332	−121.820	–	–	–	–	–	–	C
ST07	−78.639	−123.795	−13	4	43	0.70	0.0625	5 (6)	B
ST08	−77.948	−125.531	−17	5	37	0.55	0.075	6 (2)	A
ST09	−76.531	−128.473	−36	2	15	0.70	0.05	5 (0)	B
ST10	−75.814	−129.749	−39	1	11	0.90	0.05	3 (3)	B
ST12	−76.897	−123.816	−55	5	1	0.55	0.05	4 (2)	B
ST13	−77.561	−130.514	−5	3	44	0.63	0.0375	5 (2)	B
ST14	−77.838	−134.080	–	–	–	–	–	–	C
SURP	−84.720	−171.202	22	1	30	0.68	0.0375	11 (3)	A
THUR	−72.530	−97.561	73	4	−25	0.90	0.0625	5 (1)	B
UNGL	−79.775	−82.524	–	–	–	–	–	–	C
UPTW	−77.580	−109.040	−64	0.15	6	0.68	0.225	3 (1)	B
WAIS	−79.418	−111.778	−29	1	39	0.73	0.0375	13 (2)	A
WHIT	−82.682	−104.387	−58	9	17	0.78	0.225	3 (2)	B
WILS	−80.040	−80.559	−76	2	23	1.13	0.075	5 (0)	B
WNDY	−82.370	−119.413	−42	3	18	1.08	0.1125	3 (2)	B

3.2 Methods

We determine the anisotropic parameters using the widely-applied method of Silver & Chan (1991) which aims to determine the appropriate splitting parameters via the minimization of energy on the transverse component. This method analyses ground particle motion by calculating the covariance matrix of the horizontal components for all possible splitting directions and reasonable delay times. The most linear-restored particle motion, and thus the preferred fast anisotropy direction and delay time parameters for reversing the effect of simple anisotropy at a given station, are found by minimizing the magnitude of the smaller eigenvalue of the particle motion covariance matrix. The process of picking windows around the individual phases and then calculating the splitting parameters was automated using the method of Teanby *et al.* (2004). This algorithm performs splitting analysis on a range of window lengths and then finds those measurements that are stable over many different windows. These windows are then placed into clusters, with the final window chosen from the splitting analysis with the lowest error in the cluster with the lowest variance. We then evaluate the result from displays showing unrotated and rotated waveforms, the ground particle motion and the misfit contour plot for the predicted fast axis (Fig. 2).

Following the methodology of Silver & Chan (1991), the misfit contour region is constructed from the α confidence level from the following expression:

$$\frac{E_t(\phi, \delta t)}{E_t^m} \leq 1 + \frac{k}{n-k} f_{k,n-k}(1-\alpha), \quad (1)$$

where $E_t(\phi,\delta t)$ represents the n-point time-series containing the SKS phase, k represents the number of parameters (in this instance ϕ & δt), and f represents the inverse F probability distribution. For the 95 per cent confidence level $\alpha = 0.05$.

All results were individually inspected and assigned a quality rating of A, B or C based on several factors including: (1) SNR, (2) linearization of particle motion, (3) waveform coherence between the two horizontal components rotated into the fast and slow directions and (4) tightness of the misfit contours as a function of splitting parameter. To be rated as A quality, measurements had to

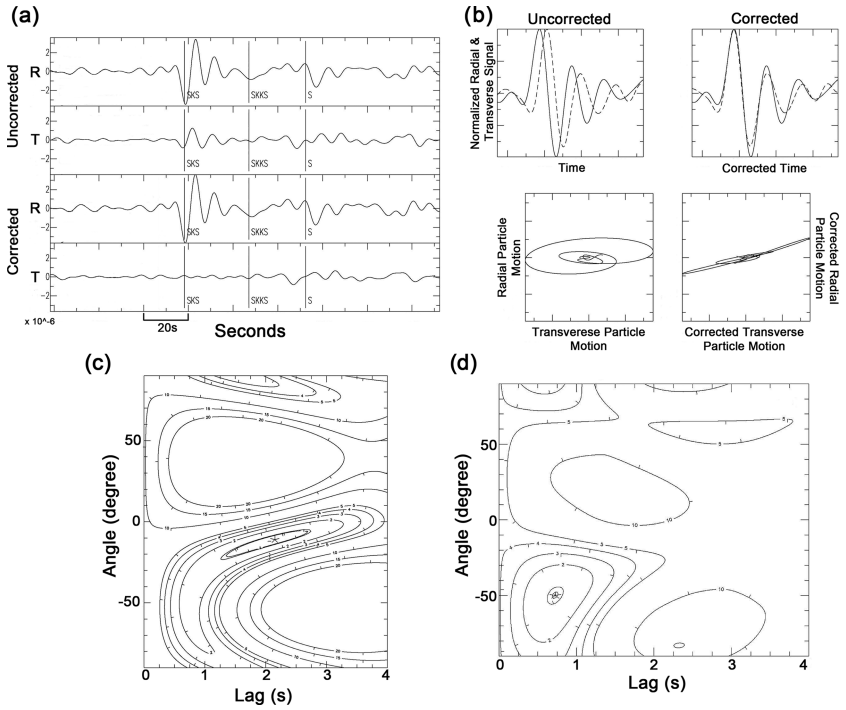

Figure 2. Example SKS splitting analysis for a single, A quality, non-null event. (a) Event processing reduces the energy on the transverse component. (b) The windowed waveforms and the particle motion plots for the raw data (left) and the data corrected for observed anisotropy (right). (c) Contour plot showing misfit as a function of splitting parameter. (d) Contour plot for the stacked solution for the station with observed anisotropy parameters. Values on the contour interval indicate the nσ value of the given contour. The contour labelled 2 indicates the 95 per cent confidence interval.

satisfy certain criteria for each of the four factors described above. Measurements had to have a SNR $>$ 8 to satisfy criterion (1). A bandpass filter was applied to noisy records with initially low SNR to improve their quality but no distinction between unfiltered and filtered records was made when judging criterion (1). To satisfy criterion (2), measurements that showed elliptical particle motion on the uncorrected seismogram had to show nearly linear particle motion on the corrected seismogram.

To be rated as B quality, measurements had to have SNR $>$ 3 to satisfy criterion (1). To satisfy criterion (2), measurements that showed elliptical particle motion on the uncorrected seismogram had to show a general reduction in ellipticity on the corrected seismograms. Criteria for A and B quality measurements for both waveform coherence and tightness of misfit contours were qualitatively judged. Only results rated B or higher were included in the final analyses.

Measurements judged to be 'null' were those that did not show energy on the transverse component, and thus a near-radially-oriented horizontal particle motion prior to analysis. Such events often yield erroneously large delay times when analysed. Null measurements can result when the initial polarization of the incoming wave is parallel or orthogonal to the fast anisotropic direction, when there is no anisotropy along the ray path, or when the SNR is low. Null measurements are most confidently captured when multiple simultaneous shear wave splitting techniques are used (i.e. the rotation-correlation method and the transverse minimization method; Wustefeld & Bokelman 2007; Long & Silver 2009). Because we utilized a single method for our shear wave splitting analysis, those measurements identified as null were not incorporated into the final stacked solution for splitting parameters. The number of null measurements observed at each station is given in Table 1.

A stacking method (Wolfe & Silver 1998) was used to increase the robustness of the results relative to analysis of individual events. This program produces a weighted sum of the individual misfit surfaces and computes a global solution for each station. Only A and B quality events were used in the stacking procedure.

Final stacked solutions for each station were assigned a quality of A, B or C based on (1) the quality of the single events included in the stack and (2) the backazimuth sampling of the station. Stations are categorized as A if the global solution consists of at least four individual measurements and are sampled only with single event ratings of A. Stations are categorized as B if the global solution consists of at least two individual measurement and is sampled only with single event ratings of A or B. A quality stations are plotted as thick vectors and B quality stations are plotted as thin vectors in Fig. 3. Stations that did not meet the above criteria were categorized as C. Note that comparison of splitting directions can be difficult in geographic coordinates for stations near the South Pole; for convenience we have also converted fast directions to the rectangular Grid coordinate system, with north oriented along the Prime Meridian and east along longitude 90° E, as is common for work near the poles. We will refer to splitting directions using this 'Grid' coordinate system in the following discussion. Both Grid and geographical directions are given in Table 1.

4 RESULTS

Stacked shear wave splitting parameters with a grade of B or better were determined for 31 out of 37 stations of the POLENET/ANET array. Six stations collected insufficient data or poor quality data and were not used in the subsequent analysis and discussion. Table 1 shows the fast direction of anisotropy, delay time and associated

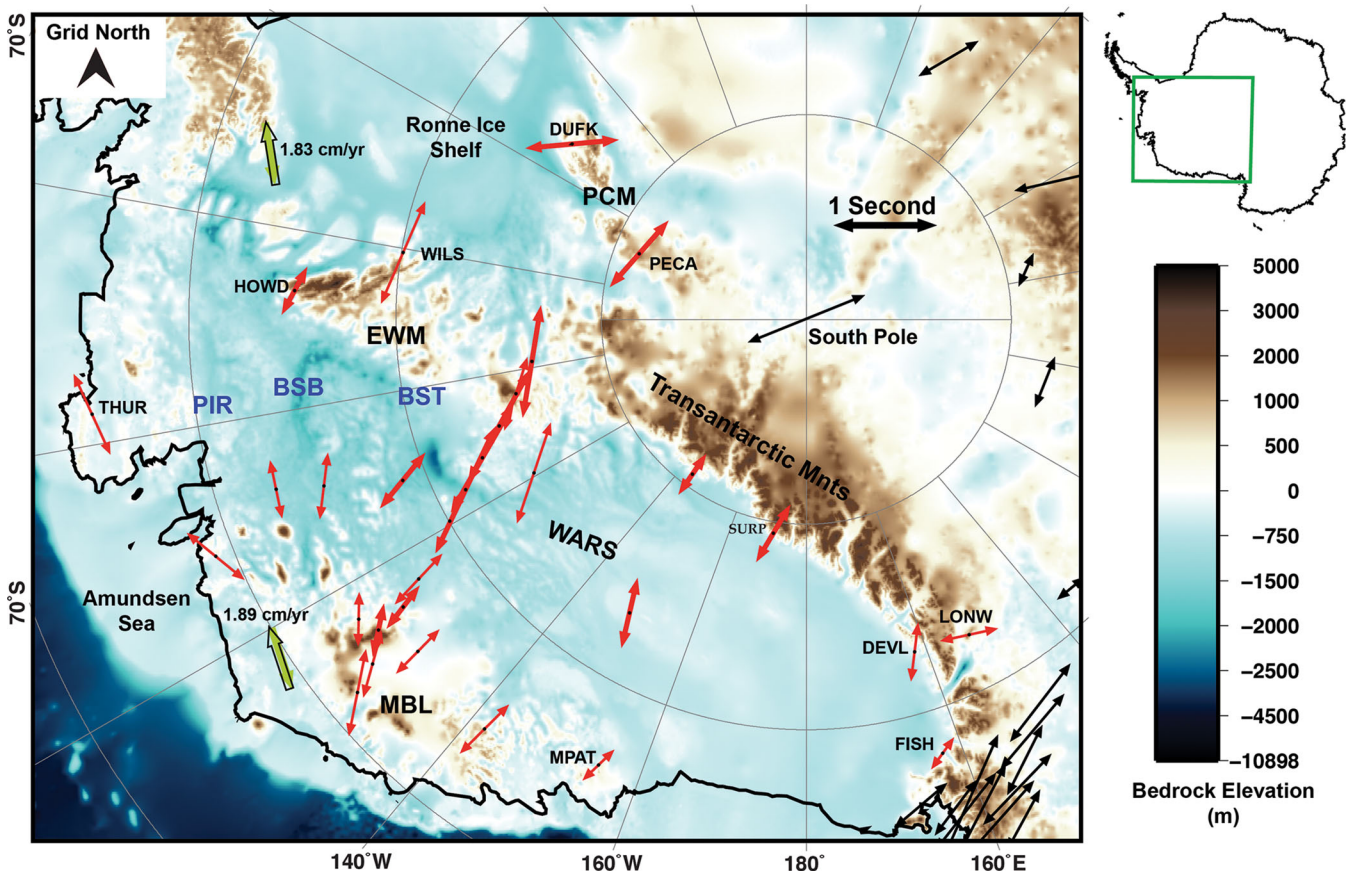

Figure 3. Splitting results for West Antarctica. The region of interest is outlined in the green box on the inset map of Antarctica. Thick red vectors represent A quality results and thin red vectors represent B quality results. Black vectors represent shear wave splitting results assembled from a variety of studies (Müller 2001; Barklage *et al.* 2009; Hernandez *et al.* 2009). Only A quality results and results from stations with multiple high quality phases were included from previous studies. Vector azimuths denote fast direction of the event stacks. The length of the vector is proportional to the splitting time, with splitting time scale indicated at right. Given the close proximity of many seismic stations, we have only labelled station names not shown in Fig. 4. Grid directions allow for simpler discussion of azimuthal values at high latitudes, and this map projection is aligned Grid N. Solid green arrows indicate the direction of Antarctic absolute plate motion in the hotspot reference frame calculated using HS3-NUVEL; at 75°S 120°W APM has an azimuth of 281.6° W and a velocity of 1.89 cm yr^{-1}. In comparison, no-net rotation reference frames calculated for the same location show APM with an azimuth of 91°E and a velocity of 1.77 cm yr^{-1}. Generally, fast directions across the West Antarctic Rift System are oriented roughly Grid NE-SW and splitting times average ∼1 s. Decreased delay times and variable fast directions are notable in the vicinity of the MBL dome and volcanic province. Background colour scale indicates bedrock elevation from Fretwell *et al.* 2013. Blue labels indicate locations of subglacial basins; PIR, Pine Island Rift; BSB, Byrd Subglacial Basin; BST, Bentley Subglacial Trench.

errors for each station. Also listed is the number of null observations and stacked events used at each station as well as the final quality rating for the station.

4.1 The TAM, EWM and PCM

The four stations located at the base of the TAM, near the boundary between the TAM and the Ross Ice Shelf (FISH, DEVL, FALL and SURP) show relatively consistent fast directions, ranging from Grid 6° to 35° (Fig. 3). The fast directions in the central TAM are oriented roughly perpendicular to the TAM front. The fast direction at FISH is consistent with fast directions found in the McMurdo Dry Valleys area by Barklage *et al.* (2009). Station LONW, located at the crest of the TAM further towards East Antarctica, shows a very different orientation of Grid 77°.

Stations located in the EWM block (HOWD, WILS, WHIT and ST01) show similar fast directions but the splitting magnitudes are variable; fast directions range from Grid 9° to 28° and delay times range from 0.55 to 1.15 s. Splitting magnitudes for the two stations located in the PCM (PECA and DUFK) are uniform and fast directions are variable. Fast directions at these locations are Grid 41° and 84° and delay times are 0.90 and 0.95 s, respectively. Both stations located in this region are A quality and are among the best constrained results due to both the number of usable events as well as the quality of those events.

4.2 The West Antarctic Rift System

Results from the seven stations located along and near the POLENET transect show extremely similar fast directions and regionally uniform splitting magnitudes (Fig. 4a). Stations ST02, ST03 and ST04 show fast directions between Grid 25° and 29° and splitting times between 1.28 and 1.43 s (Fig. 5). Together with station WNDY (Grid 18°, 1.08 s) somewhat to the west, they form an area of remarkably large and consistent splitting, indicating strong and uniform anisotropy across this region. Further north along the transect, BYRD and ST07, as well as station WAIS to the east, show similar if less tightly clustered splitting directions (Grid 22°–43°)

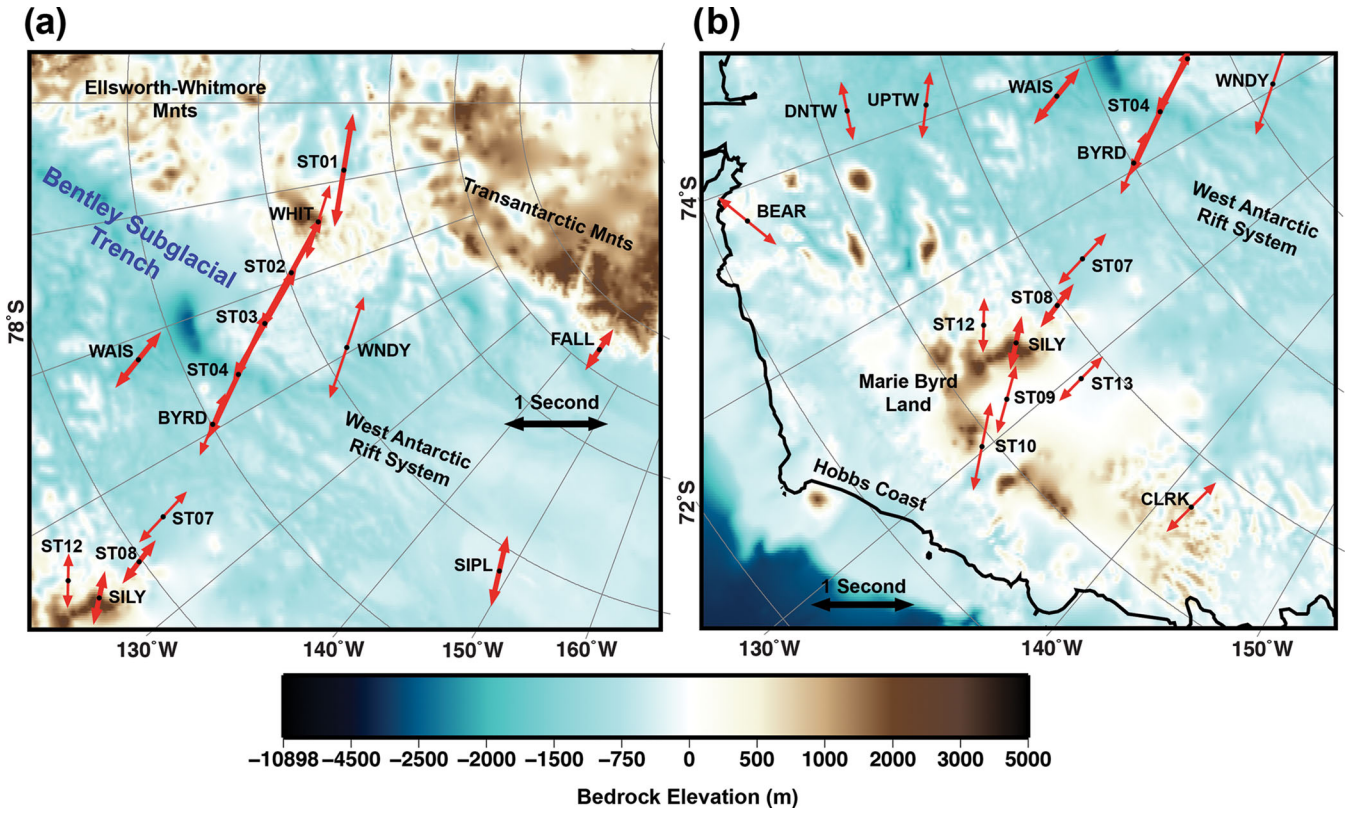

Figure 4. Splitting results from the WARS and MBL displayed as in Fig. 3. (a) Results from the POLENET WARS-crossing transect. Within the WARS, stations reveal larger splitting times with markedly uniform directions. Splitting is strongest (1.43 s) at station ST04, located over a rift basin, and weakens as stations progress coast-wards to the MBL. (b) Results from MBL can be separated into two distinct groups. Observations Grid north of the dome (SILY, ST12, ST08) have relatively small delay times (∼0.5 s) and varying fast directions. Observations on the main dome and closer to the coast (ST10; ST09) show larger delay times (>0.6 s) and a consistent fast direction that is nearly Grid N–S. Stations located Grid northwest of this region (BEAR, DNTW, UPTW) have consistent delay times (∼0.7 s) and widely varying fast directions that show a general radial pattern relative to the MBL dome.

but smaller splitting times (0.68–0.73 s). The only station located along the Siple coast, bordering the western Ross Ice Shelf (SIPL) shows a fast direction of Grid 13° and delay time of 0.73 s, very similar to that found along the transect.

Three stations (BEAR, DNTW and UPTW) are located east of the MBL dome, on the margin of and within the Thwaites Glacier and Pine Island Glacier region. These stations show consistent delay times between 0.6 and 0.75 s but widely varying fast directions (Grid −51°, −12° and 6°, respectively).

4.3 Marie Byrd Land

Overall, results across MBL show largely consistent delay times and two distinct patterns of fast directions (Fig. 4b). Delay times for the seven stations located in this region range from 0.55 to 0.90 s. The largest delay times occur near the coast and the smallest occur on the pole-ward portion of the dome, near the boundary of the WARS. Fast directions for this area can be split into two distinct groups. One set (ST09, ST10, ST12 and SILY), located near the crest of the dome, shows fast directions clustered between Grid 1° and 15°. The second set of stations (ST08, ST13 and CLRK), located south and west of the dome, display fast directions between Grid 37° and 45°. The station MPAT, located approximately where the Siple Coast, Ross Ice Shelf and the Pacific coast come together, is east of the MBL dome yet still within the MBL crustal block and shows a similar splitting direction (Grid 45°) with a smaller splitting time (0.45 s).

5 DISCUSSION

5.1 Depth extent of the observed anisotropy

It is well recognized that the depth resolution of core phase splitting measurements is poor due to the path-integrated nature of the measurements and the steep ray path incidence angles of core phases. Tight constraints on the depth distribution of anisotropy can be inferred from short period lateral variations via Fresnel zone arguments whereby the depth of anisotropy is limited to regions where Fresnel zones corresponding to different splitting observations should not overlap (Alsina & Sneider 1995). However, it is also well established that anisotropic signals observed in teleseismic shear wave splitting studies such as this primarily reflect anisotropy in the upper mantle. Shallow sources of anisotropy may be produced from aligned cracks and microcracks, or fabric, in the upper 10–15 km of the crust. However, crustal shear wave splitting measurements generally range between 0.05 and 0.2 s (e.g. Aster *et al.* 1990; Savage 1999) and do not strongly affect the typically much larger mantle anisotropy signatures for SKS signals. Furthermore, this region is characterized by thin crust, generally 35 km or less, which would likely be unable to accumulate an appreciable fraction of the observed delay times (Winberry & Anandakrishnan 2004; Chaput *et al.* 2014). Barruol & Mainprice (1993) showed that in extreme cases where the entire crust is composed of anisotropic material with steeply dipping foliations, the crustal signature of anisotropy could reach up to 0.5 s. However, the complex tectonic

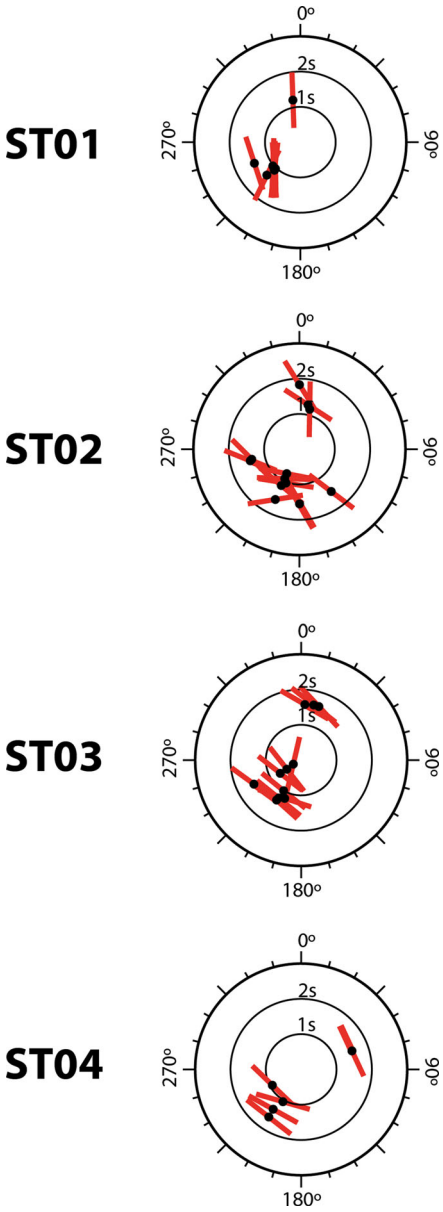

Figure 5. Individual splitting results for all events stacked in the final solution for A-quality stations along the northern portion of the POLENET transect (ST01, ST02, ST03, ST04). The BAZ of the event is represented by angle clockwise from 0°, the delay time by the radial distance from the origin of the plot, and the direction of the fast axis by the azimuth of the red vector. Individual splitting results for the remaining stations are available in the supplementary material.

history of the region suggests that retention of such large-scale coherent crustal structure would be difficult. Growing evidence suggests that anisotropy may be present in the lower mantle and at the core-mantle boundary (e.g. Garnero *et al.* 2004; Panning & Romanowicz 2006). However, consistency in splitting parameters between rays with different backazimuths (thus different sampling regions of the lower mantle) strongly suggests that such effects do not contribute appreciably to these observations. Individual plots of backazimuth against fast axis and delay time are included in the Supporting Information, a subset of the stations are shown in Fig. 5. Our final measurements are produced by stacking arrivals from a variety of backazimuths when available, so that any bias from mid- or lower mantle anisotropy along a particular azimuth should be down-weighted in the final, averaged result.

5.2 Relationship of anisotropy to absolute plate motion over the mantle

The motion of plates over the mantle may induce asthenospheric shear strain beneath the plate with the axis of shear aligned in the direction of plate motion relative to the ambient mantle (e.g. Wang *et al.* 2008). This plate basal shear mantle deformation mechanism should cause seismic anisotropy such that the olivine fast axis becomes oriented in the direction of plate motion in an absolute mantle reference frame, thus producing fast anisotropy directions parallel to absolute plate motion (APM; e.g. Savage 1999). However, the fast anisotropic directions from the splitting measurements consistently show large angles with APM directions in both no-net-rotation (NNR) and hotspot (HS) absolute reference frames (Argus *et al.* 2010; Fig. 3). The NNR frame represents the plate velocity relative to the weighted average of all the plate velocities on the earth's surface (Argus & Gordon 1991). In comparison, the HS reference frame minimizes the movement of hotspots, and its use as an absolute reference frame assumes that hotspots are fixed relative to the lower mantle (e.g. Minster *et al.* 1974). The inferred basal shear direction for both HS and NNR absolute reference frames is highly inconsistent with most of the observed splitting results, with the exception of a few far Grid west sites (e.g. THUR and DNTW). This suggests that the anisotropic fabric does not broadly result from shear associated with the motion of Antarctic lithosphere over the mantle. The lack of signal from Antarctica motion relative to the mantle is not surprising seeing that Antarctica moves slowly in both the NNR (1.77 cm yr^{-1} in a direction of 91.2°E) and HS (1.89 cm yr^{-1} in a direction of 281.6°W) reference frames. Debayle & Yanick (2013) note that only fast moving plates (velocity >4 cm yr^{-1}) produce sufficient shearing at their base to organize anisotropy within the asthenosphere beneath the entire tectonic plate. Further, beneath slow moving plates (like Antarctica), plate motion is predicted to only partially control mantle asthenospheric flow, given that the uppermost mantle is subject to other secondary convection mechanisms.

5.3 Anisotropy in East Antarctica versus West Antarctica

Splitting results from West Antarctica are highly distinct from those reported for East Antarctica, particularly compared to the South Pole region and the East Antarctic highlands (Müller 2001; Bayer *et al.* 2007; Reading & Heintz 2008; Barklage *et al.* 2009; Fig. 6). Fast directions reported from the PCM and along the TAM (e.g. DUFK, PECA and LONW) are also distinct from the overall Grid NE–SW direction seen across much of West Antarctica. Mantle shear velocity maps show that these three stations lie outside of the low velocity upper mantle that underlies most of West Antarctica (e.g. Heeszel *et al.* 2011; Fig. 7). These patterns are consistent with the dissimilar tectonic conditions across Antarctica, whereby East Antarctica represents a stable continental craton underlain by thick continental lithosphere (Heeszel *et al.* 2011) and West Antarctica is composed of crustal blocks that have undergone Mesozoic and Cenozoic tectonism, with a relatively hot, shallow mantle asthenosphere. Potentially, the disparate splitting patterns reflect large-scale deflection of mantle flow around the East Antarctic craton. This mechanism has been suggested for other locations in close proximity to cratons (e.g. Clitheroe & van der Hilst 1998; Walker *et al.* 2004; Miller

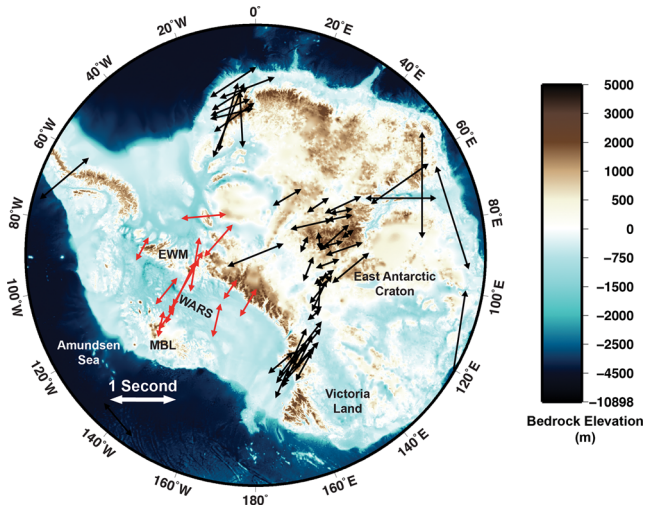

Figure 6. Antarctica, showing splitting vectors from this and a variety of other studies (Müller 2001; Bayer *et al.* 2007; Usui *et al.* 2007; Reading & Heinz 2008; Barklage *et al.* 2009; Hernandez *et al.* 2009). Only results from stations with multiple high-quality observations were plotted. Background colour scale indicates bedrock elevation from Fretwell *et al.* 2013.

et al. 2013). In this scenario, asthenospheric flow is directed around the edge of the cratonic keel rather than beneath it, leading to fast directions oriented approximately parallel to the craton edge (Fouch *et al.* 2000; Miller & Becker 2012). However, splitting results from the boundary of the East Antarctic craton are oriented normal rather than parallel to the margin, suggesting that simple edge driven flow cannot explain the observations. Further, the small magnitude APM reported for Antarctica and absence of vigorous mantle flow due to large-scale tectonics likely results in insufficient shearing within the asthenosphere needed to coherently deflect flow around the cratonic keel (Miller & Becker 2012; Miller *et al.* 2013). These observations suggest that, as is observed in other cratonic regions, the splitting of East Antarctica results largely from anisotropy frozen into thick and cold continental lithosphere (e.g. Barklage *et al.* 2009), whereas splitting seen in most of West Antarctica largely results from asthenospheric fabric that reflects recent and ongoing mantle processes. As discussed below, the same interpretation may not be valid for the EWM crustal block.

5.4 WARS anisotropy resulting from Cenozoic extension

5.4.1 Extension induced mantle anisotropy

It is well accepted that rift systems develop via extension and ultimately rupture of thick continental lithosphere, however, the mechanisms that control the character and style of rifting remain contentious. Specifically, a new model of rift development in which magmatic products (i.e. dikes and magma-filled lenses) accommodate a considerable proportion of extension (e.g. Buck 2004; Thybo & Neilson 2009; Bialis *et al.* 2010) has been offered up in contrast to previous models of passive rifting (i.e. extension driven by far field stresses). Simple 2-D orthogonal extension in the mantle lithosphere associated with plate stretching should produce olivine LPO and shear wave azimuthal anisotropy in the direction of extension (McKenzie 1979; Blackman *et al.* 1996; Vauchez *et al.* 2000). However, due to the conflicting effects of strain accumulation and lithospheric thinning, this signal is expected to be weak. Extension-parallel fast directions have been reported for multiple continental rift systems (Vinnik *et al.* 1992; Gao *et al.* 1997) and portions of the Basin and Range (Obrebski *et al.* 2006; Xue & Allen 2006), one of the few continental extensional systems of similar size and scale to the WARS. Studies at oceanic spreading centres also report extension parallel fast axes which are likely due to flow induced LPO of anisotropic minerals within the asthenospheric mantle (e.g. Blackman & Kendall 1997; Wolfe & Solomon 1998).

Conversely, if extension is accommodated largely by magmatic intrusion, splitting fast directions will align parallel to strike of the bodies and hence be rotated 90° to the direction of shearing. Studies of the Main Ethiopian Rift, the northernmost portion of the East African rift system (EARS), reveal shear-wave-splitting directions aligned parallel to the rift axes indicative of the presence of oriented melt pockets in the uppermost mantle and crust (Walker *et al.* 2004; Kendall *et al.* 2005) or alternatively indicating large-scale, oriented mantle flow in the presence of a superplume (Bagley & Nyblade 2013).

Recently, Eilon *et al.* (2014) reported extension parallel fast axes with large delay times (>1 s) from the highly extended continent within the Woodlark Rift. They suggest that the anisotropic signal there represents extension driven LPO of olivine within the asthenospheric mantle similar to mechanisms inferred at mid-ocean ridges. Further, they propose that the anisotropic fabric within highly extended continental rift regimes may characterize a transition from small-strain continental rifts (where fast axes may be expected to parallel the strike of melt bodies and hence the rift axis) to mid-ocean ridges (where fast axes parallel the extension direction).

5.4.2 Anisotropic signature of Cenozoic WARS extension

Rifting within the Ross Sea sector of the WARS during the Eocene and Oligocene was multiphase with extension occurring largely transcurrently with isolated periods and locations of orthogonal extension (Wilson 1995; Miller *et al.* 2001, Granot *et al.* 2013). Poles of East Antarctica–West Antarctica rotation for that time period (40–26 Ma) are located in central West Antarctica and suggest that the western sector of the WARS and specifically the locations of the remarkably deep subglacial basins (i.e. Pine Island Rift and the Bentley Trench) underwent a significant period of oblique convergence (Granot *et al.* 2013). These poles predict roughly east-west convergence in the vicinity of the POLENET transect, which is at large angles to the observed fast directions. This indicates that the anisotropy is not correlated with the inferred transcurrent and convergent deformation during Eocene–Oligocene time in the central and southern WARS.

Limited extension within the Adare Basin (northern WARS), coeval with the opening of the Terror Rift (Henrys *et al.* 2007; Fielding *et al.* 2008) during the mid-Miocene, suggests that a major change in relative plate motion between East and West Antarctica occurred at ∼17 Ma. This change in tectonic framework is proposed to be concomitant with the final pulse of extension within the WARS where rifting increased towards the interior of the WARS (Granot *et al.* 2010). The WARS extension direction during this final pulse of rifting is not known, as magnetic anomalies in the Adare Trough do not allow a pole of rotation to be calculated for this time period (Granot *et al.* 2010). However, it is a reasonable assumption that the extension would have been orthogonal or at high angle to well developed rift structures in the Pine Island Glacier basin and Bentley Trench.

Fast directions along and near the POLENET transect in the WARS are seen to indeed be oriented approximately orthogonal

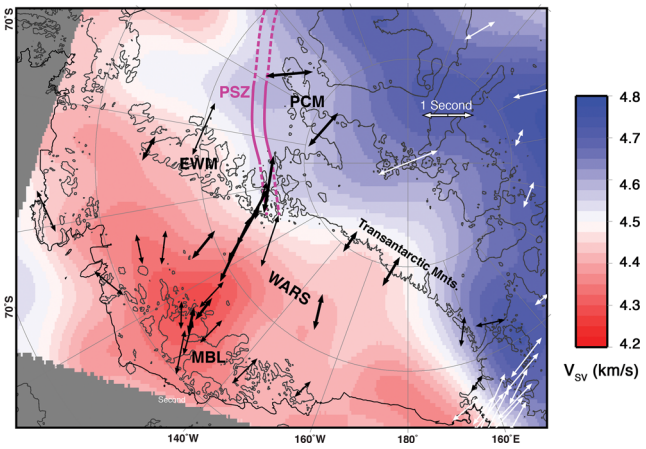

Figure 7. *S*-wave velocity variation at 180 km depth (after Heeszel *et al.* 2011) with splitting parameters from this study in black and previous studies (Müller 2001; Barklage *et al.* 2009; Hernandez *et al.* 2009) in white. The boundary of the Pagano Shear Zone (PSZ; Jordan *et al.* 2013) are represented by the purple solid and dashed lines; solid line indicates where the PSZ has been identified from aerogeophysical data, dashed line indicates inferred continuation of the PSZ towards West and East Antarctica, respectively. The lowest velocity region directly underlies the MBL dome, and the highest velocities are found across the TAM and into the East Antarctic craton.

to the topographic axis of the Bentley Trench (Fig. 4). The largest splitting time (1.43 s) occurs at station ST04, which is located above the Bentley Trench and also shows the smallest crustal thickness (21 km) and greatest amount of crustal thinning along the transect (Chaput *et al.* 2014). The delay times decrease coast-wards along the transect towards MBL, consistent with higher elevation, thicker crust and decreasing extension (Chaput *et al.* 2014). This preliminarily suggests that the anisotropy across this region results from deformational fabric accrued during the last (Neogene) phase of strong WARS rifting, potentially focused within the Bentley Trench.

Splitting measurements towards the Pine Island Glacier region (UPTW, DNTW, BEAR, THUR) do not show a similar correspondence between fast directions and the inferred extension direction. This may be partly due to the complex tectonic history in this region; Eocene-Oligocene rotation poles predict increasing convergence in this direction and Granot *et al.* (2013) proposed that Pine Island and other present rift basins were transform fault features at that time. Some of the fast directions (e.g. DNTW) are oriented approximately in the expected shear direction of these transform faults. Alternatively, fast directions in this region may be related to radial flow associated with the MBL plume, as discussed in Section 5.6.

If continental extension produces mantle anisotropy with strong extension-parallel fast directions in West Antarctica, an important question is why are similar extension parallel orientations not found at some other prominent continental rift zones such as the EARS? Along-strike fast directions in the EARS are hypothesized to be due to SPO anisotropy due to melt-filled extensional cracks (Walker *et al.* 2004; Kendall *et al.* 2005) and/or to large-scale along-strike flow from the African superplume (Bagley & Nyblade 2013). The African superplume explanation suggests that perhaps the East Africa observations cannot be generalized to other continental rifts. Melt-filled cracks are certainly a possibility in any extensional region, but most evidence suggests that the WARS is not currently undergoing significant extension (Donnellan & Luyendyk 2004; Winberry & Anandakrishnan 2004; Wilson *et al.* 2011), whereas the East African Rift is currently extending at rates of up to 6 mm yr^{-1} (Stamps *et al.* 2008).

We alternatively suggest that the anisotropic signature observed within the WARS was jointly imparted to the lithosphere and asthenosphere via ductile shearing associated with the large-magnitude extension between East and West Antarctica. Deformation within the lithosphere and asthenosphere leading to the accumulation of pervasive anisotropy likely dominated over competing mechanisms like lithospheric thinning which would have otherwise acted to obstruct the retention of a coherent anisotropic fabric. This is in good agreement with the study of Eilon *et al.* (2014) which suggested that extension parallel fast axes within the highly extended Woodlark Rift in Papua New Guinea represent widespread coherent anisotropic fabric within the asthenosphere accumulated via extension controlled LPO. They point out that the observation of extension parallel fast axes with large delay times (>1 s) beneath highly extended continental rifts represent mantle anisotropic fabrics dominated by flow produced LPO rather than fabrics characterized by melt or pre-existing structure. We suggest that the anisotropy observed within the WARS resulted from extensive Cenozoic extension including the final pulse of western WARS rifting in the Miocene, the signature of which has since been preserved within the asthenospheric mantle owing to the weak influence of shear from small-magnitude APM associated with Antarctica.

5.5 Anisotropy resulting from the rotation of the Ellsworth-Whitmore crustal block

Splitting parameters in the EWM are consistent with results from the adjacent stations in the WARS potentially suggesting that the same extensional mantle deformational fabric producing the strong anisotropy in the WARS extends beneath the EWM block. However, mantle shear velocities in the region are higher beneath the EWM than the rest of West Antarctica, suggesting the EWM, as indicated by the geology and palaeomagnetic data, may be underlain by older continental lithosphere not present within the WARS (Heeszel *et al.* 2011; Lloyd *et al.* 2013; Fig. 7). Further, mantle seismic velocities found in the EWM are significantly lower than those for the East Antarctic craton or even the PCM region, suggesting nonetheless some tectonic modification of the continental lithosphere. Combined this evidence suggests that the translocation and rotation of the EWM likely induced additional deformation and alteration of the continental lithosphere compared to the surrounding regions.

Alternatively, splitting parameters in the EWM region may reflect deformation due to shear motion within the long inferred (Storey & Dalziel 1987) and recently aeromagnetically imaged Pagano Shear Zone (PSZ), a major left-lateral strike-slip fault system between East and West Antarctica (Jordan *et al.* 2013; Fig. 7). The PSZ strikes approximately Grid NE-SW at the juncture of the EWM and the TAM. Elongate, structurally controlled Jurassic granite intrusions along the flanks of the PSZ suggest that the fault system accommodated motion primarily during the Mesozoic. Gravity and magnetic anomaly mapping show no evidence for a connection between the Mesozoic rifting events and the Cenozoic WARS rifting, although the Early Jurassic Ferrar-Karoo Large Igneous Province suggests rifting in the WARS may have originated at that time. Additionally, shear velocity maps reveal that the PSZ boundary, imaged by Jordan *et al.* (2013), sits exactly along the boundary between the fast velocities in East Antarctica and the slow velocities in West Antarctica (Fig. 7). Results from ST01, located within the PSZ, show fast axes subparallel to the proposed strike of the PSZ and dissimilar from observations along the remainder of the POLENET transect (Fig. 5). Thus, anisotropic fabric beneath the PSZ may be

representative of Mesozoic shearing from this feature. In contrast, in the simplest interpretation, anisotropy within the larger EWM results from mantle deformation associated with the same Neogene large-scale extensional processes that produced the WARS which is either coincidentally aligned with, or has been sufficient to overprint, prior deformation associated with the tectonic history of the block.

Additionally, a third possibility exists. While details of the tectonic history of the EWM remain enigmatic it is now largely accepted that this tectonic block originated adjacent to the South African Cape Fold Belt prior to Gondwana breakup (e.g. Dalziel 2007) and has translated and rotated as a microplate. In this scenario, the EWM crustal block rotated as much as 90° counterclockwise relative to East Antarctica (Grunow *et al.* 1987; Randall & Niocaill 2004) and was laterally translated to its present day position at the head of the Weddell Sea embayment. Fast anisotropic directions in this crustal block are consistently oriented at approximately Grid 25°, similar to splitting directions in the WARS, and systematically different from results in the PCM. The EWM splitting directions may represent anisotropy frozen into the continental lithosphere of the EWM block, which would have originally been parallel with PCM lithospheric anisotropy. The azimuths of the splitting directions in the EWM crustal block and in the PCM are in each case a few degrees clockwise with respect to the strike of the early Mesozoic Gondwanide structural trends. This suggests that restoration of the EWM crustal block within a reconstruction of the Gondwana supercontinent would bring them into parallelism, implying the anisotropy in the EWM crustal block may have been 'frozen' into the lithosphere prior to breakup of the supercontinent.

5.6 Anisotropy resulting from a mantle plume

MBL exhibits splitting times and directions that depart systematically and are locally discordant with observations within the WARS and TAM. Mantle shear velocity maps highlight an upper mantle low velocity region associated with the MBL, and suggest that splitting in this region may represent processes associated with a MBL mantle plume (Heeszel *et al.* 2011). Models for anisotropy at mantle plumes suggest that fast anisotropic directions should be oriented vertically within the central upwelling and radially within the expanding plume head (e.g. Rümpker & Silver 2000; Xue & Allen 2005). With the superimposed influence from absolute plate motion, horizontal flow away from the central plume head upwelling is predicted to be parabolic (Walker *et al.* 2005). Conversely, recent experimental studies suggest that despite radially outward flow of material within the plume head, olivine fast axes will coherently align perpendicular to the flow in an azimuthal pattern. Specifically, it is proposed that the interchange between radial shortening and azimuthal stretching within the expanding plume head induces extensional pure strain, thus locking the crystalline alignment into a flow normal orientation (Druken *et al.*, in preparation).

Anisotropy within the central upwelling of the MBL hot spot should be weak with small delay times and varied fast directions due to the vertical orientation of the olivine crystals. Splitting above the eastern MBL dome is indeed small in magnitude (delay times average ∼0.6 s) in comparison to those observed in the WARS yet shows a consistent fast direction (e.g. ST13, CLRK, ST08) of ∼40°. Mantle xenoliths from MBL indicate that portions of the sampled lithospheric mantle have minimum ages of 1.3–1.5 Ga (Handler *et al.* 2003). Thus, the thicker MBL crust and/or the preservation of MBL Proterozoic lithosphere implies that consistent fast directions in this region may represent an older signature of anisotropy that has been 'frozen into' the lithospheric mantle prior to the onset of plume activity and Mesozoic-Cenozoic extension.

Anisotropy outside of the proposed plume axis, but influenced by plume head processes should show fast axes oriented either parallel or normal to radial flow from the proposed plume head. However, only partial indications of a radially or flow normal oriented pattern of fast directions is observed. Results from the Amundsen Sea region (BEAR, DNTW, UPTW, WAIS) are consistent in delay time (∼0.75 s) and have fast directions that are approximately radially oriented with respect to the central MBL dome. Shear velocity maps of the region at depth further emphasize the spatial relationship between the radial anisotropic pattern and the low upper mantle velocities extending Grid northwest from the centre of the MBL dome (Heeszel *et al.* 2011; Fig. 7). However, this radial pattern of anisotropic directions is not reported at stations Grid southeast of MBL (e.g. CLRK, MPAT), which display fast directions that are subparallel to those observed along the central TAM and within the WARS, where upper mantle shear velocities are somewhat higher.

6 CONCLUSIONS

Core phase-derived splitting results from West Antarctica generally show a large number of stations with distinct (∼1 s) anisotropy and fast axes oriented Grid NE–SW, orthogonal to the trend of the TAM. We suggest that anisotropy in this region is strongly influenced by mantle fabrics that were established during Cenozoic WARS extension, crustal thinning and associated mantle flow. Specifically, splitting along the relatively dense transect of POLENET/ANET seismic stations within the WARS (between the MBL dome and the EWM) is subparallel to the apparent direction of Neogene WARS extension, indicating the absence of partial melt or other influences within the rift system that would result in a rift axis parallel or oblique fast direction trends. Rather, plate stretching within the highly extended WARS led to the accumulation of pervasive anisotropic fabrics within the uppermost mantle and dominated over competing processes like lithospheric thinning which would have otherwise hindered the retention of a widespread, coherent anisotropic signal. The weak influence of shear from small-magnitude APM likely allowed for the preservation of such widespread coherent fabric after WARS extension shut down.

Multiple hypotheses exist to explain the pattern of splitting within the EWM crustal block. Broadly the EWM microplate shows anisotropy that is consistent with the WARS, suggesting either coincident underlying alignment with WARS trends or underlying mantle that has participated in WARS-oriented flow. Alternatively, the anisotropic fabric may be related to the deformation within the PSZ between the East Antarctic craton and the EWM block or perhaps be evidence for fabric frozen into the mantle lithosphere prior to fragmentation of the Gondwanaland supercontinent. Although the observations are ambiguous, weaker splitting parameters observed at the MBL dome are compatible with less pervasive Cenozoic extension and somewhat thicker lithosphere, or with variable splitting associated with upper mantle plume and plume head influences. Fast directions in the Amundsen Sea region are approximately radial to the MBL dome and may indicate a mantle flow pattern away from the dome, or less clearly, from the complicated Cenozoic tectonics associated with Eocene-Oligocene convergence followed by Neogene extension responsible for the formation of extremely deep subglacial basins and troughs in the region.

ACKNOWLEDGEMENTS

We thank Patrick Shore from Washington University, Tim Parker, Brian Bonnett, Guy Tytgat, Paul Carpenter from the IRIS PASSCAL Instrument Center and many other individuals for field and technical assistance in acquiring POLENET data. We thank Nick Teanby for use of his shear wave splitting analysis code. We thank Tom Jordan for productive discussion concerning the Pagano Shear Zone. Finally, we thank two anonymous reviewers for constructive comments that improved this manuscript. Seismic instrumentation provided and supported by the Incorporated Research Institutions for Seismology (IRIS) through the PASSCAL Instrument Center at New Mexico Tech. Seismic data are available through the IRIS Data Management Center. The facilities of the IRIS Consortium are supported by the National Science Foundation under Cooperative Agreement EAR-1063471, by NSF Polar Programs and the DOE National Nuclear Secuxstrity Administration. This research was funded by the National Science Foundation under grants ANT-0632209, ANT-0632185 and ANT-0632330.

REFERENCES

Alsina, D. & Snieder, R., 1995. Small-scale sublithospheric mantle deformation: constraints from SKS splitting observations, *Geophys. J. Int.,* **123,** 431–448.

Anderson, J.B., 1999. *Antarctic Marine Geology,* pp. 28–57, Cambridge Univ. Press.

Argus, D.F. & Gordon, R.G., 1991. No-net-rotation model of current plate velocities incorporating plate motion model NUVEL-1, *Geophys. Res. Lett.,* **18**(11), 2039–2042.

Argus, D.F., Gordon, R.G., Heflin, M.B., Ma, C., Eanes, R.J., Willis, P., Peltier, W.R. & Owen, S.E., 2010. The angular velocities of the plates and the velocity of Earth's center from space geodesy, *Geophys. J. Int.,* **180**(3), 913–960.

Aster, R., Shearer, P. & Berger, J., 1990. Quantitative measurements of shear-wave polarizations at the Anza seismic network, southern California – implications for shear-wave splitting and earthquake prediction, *J. geophys. Res.,* **95,** 12 449–12 474.

Bagley, B. & Nyblade, A.A., 2013. Seismic anisotropy in eastern Africa, mantle flow, and the African superplume, *Geophys. Res. Lett.,* **40,** 1–6.

Balestrieri, M.L., Bigazzi, G., Ghezzo, C. & Lombardo, B., 1994. Fission track dating from Granite Harbor Intrusive Suite and uplift-denudation history of the Transantarctic Mountains in the area between the Mariner and David Glaciers (Northern Victoria Land, Antarctica), *Terra Antarc.,* **1**, 82–87.

Barklage, M., Wiens, D.A., Nyblade, A. & Anandakrishnan, S., 2009. Upper mantle seismic anisotropy of South Victoria Land and the Ross Sea coast, Antarctica from SKS and SKKS splitting analysis, *Geophys. J. Int.,* **178,** 729–741.

Barruol, G. & Mainprice, D., 1993. A quantitative evaluation of the contribution of crustal rocks to the shear-wave splitting of teleseismic SKS waves, *Earth planet. Sci. Lett.,* **78,** 281–300.

Bayer, B., Müller, C., Eaton, D.W. & Jokat, W., 2007. Seismic anisotropy beneath Dronning Maud Land, Antarctica, revealed by shear wave splitting, *Geophys. J. Int.,* **171,** 339–351.

Behrendt, J., 1999. Crustal and lithospheric structure of the West Antarctic rift system from geophysical investigations – a review, *Global Planet. Change,* **23**(1–4), 25–44.

Behrendt, J.C. & Cooper, A.K., 1994. Evidence of rapid Cenzoic uplift of the shoulder of the West Antarctic rift system and a speculation on possible climate forcing, *Geology,* **19,** 315–319.

Behrendt, J.C., LeMasurier, W.E., Cooper, A.K., Tessensohn, F., Trehu, A. & Damaske, D., 1991. Geophysical studies of the West Antarctic rift system, *Tectonics,* **10,** 1257–1273.

Behrendt, J.C., Saltus, R., Damaske, D., McCafferty, A., Finn, C.A., Blankenship, D. & Bell, R.E., 1996. Patterns of Late Cenozoic volcanic and tectonic activity in the West Antarctic rift system revealed by aeromagnetic surveys, *Tectonics,* **15,** 660–676.

Bialas, R.W., Buck, W.R., Studinger, M. & Fitzgerald, P., 2007. Plateau Collapse model for the Transantarctic Mountains/West Antarctic rift system: insights from numerical experiments, *Geology,* **35**(8), 687–690.

Bialis, R.W., Buck, W.P. & Qin, R., 2010. How much magma is required to rift a continent? *Earth planet. Sci. Lett.,* **292,** 68–78.

Bingham, R.G., Ferraccioli, F., King, E.C., Larter, R.D., Pritchard, H.D., Smith, A.M. & Vaughan, D.G., 2012. Inland thinning of the West Antarctic Ice Sheet steered along subglacial rifts, *Nature,* **487,** 468–471.

Blackman, D.K., Von Herzen, R.P. & Lawver, L.A., 1987. Heat flow and tectonics in the western Ross Sea, Antarctica, *Earth Sci. Ser.,* **5B,** 179–189.

Blackman, D.K. & Kendall, J.M., 1997. Sensitivity of teleseismic body waves to mineral texture and melt in the mantle beneath a mid-ocean ridge, *Phil. Trans. R. Soc. Lond., A,* **355,** 217–231.

Blackman, D.K., Kendall, J.M., Dawson, P.R., Wenk, H.R., Boyce, D. & Morgan, J.P., 1996. Teleseismic imaging of subaxial flow at mid-ocean ridges: traveltime effects of anisotropic mineral texture in the mantle, *Geophys. J. Int.,* **127,** 415–426.

Borg, S.C., DePaolo, D.J. & Smith, B.M., 1990. Isotopic structure and tectonics of the central Transantarctic Mountains, *J. geophys. Res.,* **95,** 6647–6667.

Bradshaw, J.D., 1989. Cretaceous geotectonic patterns in the New Zealand region, *Tectonics,* **8**(4), 803–820.

Buck, W.R., 2004. Consequences of asthenospheric variability on continental rifting, in *Rheology and Deformation of the Lithosphere at Continental Margins,* eds Karner, G.D., Taylor, B., Driscoll, N.W. & Kohlstedt, D.L., pp. 1–30, Columbia Univ. Press.

Busetti, M., Spadini, G., van der Wateren, F.M., Cloetingh, C. & Zonolla, C., 1999. Kinematic modeling of the West Antarctic rift system, Ross Sea, Antarctica, *Global Planet. Change,* **23,** 79–103.

Cande, S.C., Stock, J.M., Mueller, R.D. & Ishihara, T., 2000. Cenozoic motion between east and West Antarctica, *Nature,* **404,** 145–150.

Chaput, J. *et al.*, 2014. Crustal thickness across West Antarctica, *J. geophys. Res.,* **119,** 1–18.

Clarkson, P.D. & Brook, M., 1977. Age and position of the Ellsworth Mountains crustal fragment, Antarctica, *Nature,* **265**(5595), 615–616.

Clitheroe, G. & van der Hilst, R.D., 1998. Complex anisotropy in the Australian lithosphere from shear-wave splitting in broad-band SKS records, in *Structure and Evolution of the Australian Continent,* Geodyn. Ser., vol. 26, Braun, J. *et al.* pp. 73–78, AGU, Washington, D.C.

Clow, G.D. & Cuffey, K.M., 2012. High heat-flow beneath the central portion of the West Antarctic ice sheet, Abstract C31A-0577 presented at 2012 Fall Meeting, AGU, San Francisco, CA, 3–7 Dec.

Curtis, M.L., 2001. Tectonic history of the Ellsworth Mountains, West Antarctica: reconciling a Gondwana enigma, *Geol. Soc. Am. Bull.,* **113**(7), 939–958.

Dalziel, I.W.D., 1992. Antarctica; a tale of two supercontinents, *Ann. Res. Earth planet. Sci.,* **201,** 501–526.

Dalziel, I.W.D., 2007. The Ellsworth Mountains: critical and enduringly enigmatic, *Antarctica: A Keystone in a Changing World—Online Proceedings of the 10th ISAES,* eds Cooper, A.K. & Raymond, C.R. *et al.*, U.S. Geol. Surv. Open-File Rep. 2007–1047, Short Research Paper 004, Santa Barbara, CA.

Dalziel, I.W.D. & Elliot, D.H., 1982. West Antarctica: problem child of Gondwanaland, *Tectonics,* **1,** 3–19.

Debayle, E. & Yanick, R., 2013. Seismic observations of large-scale deformation at the bottom of fast-moving plates, *Earth planet. Sci. Lett.,* **376,** 165–177.

Donnellan, A. & Luyendyk, B.P., 2004. GPS evidence for a coherent Antarctic plate and for postglacial rebound in Marie Byrd Land, *Global Planet. Change,* **42**(1–4), 305–311.

Dunbar, N.W., McIntosh, W.C. & Esser, R.P., 2008. Physical setting and tephrochronology of the summit caldera ice record at Mount Moulton, West Antarctica, *Geol. Soc. Am. Bull.,* **120**(7–8), 796–812.

Eilon, Z., Abers, G.A., Jin, G. & Gaherty, J.B., 2014. Anisotropy beneath a highly extended continental rift, *Geochem. Geophys. Geosyst.,* **15,** 545–564.

Fielding, C.R., Whittaker, J., Henrys, S.A., Wilson, T.J. & Naish, T.R., 2008. Seismic facies and stratigraphy of the Cenozoic succession in McMurdo sound, Antarctica: implications for tectonic, climatic and glacial history, *Palaeogeog. Palaeclimat. Palaeoecol.,* **260,** 8–29.

Finn, C.A., Mueller, R.D. & Panter, K.S., 2005. A Cenozoic diffuse alkaline magmatic province (DAMP) in the southwest pacific without rift or plume origin, *Geochem. Geophys. Geosyst.,* **6,** 26–26.

Fischer, K.M., Fouch, M.J., Wiens, D.A. & Boettcher, M.S., 1998. Anisotropy and flow in Pacific subduction zone back-arcs, *Pure appl. Geophys.,* **151,** 463–475.

Fitzgerald, P.G., 1992. The Transantarctic Mountains of southern Victoria Land: the application of apatite fission track analysis to a rift shoulder uplift, *Tectonics,* **11,** 634–662.

Fitzgerald, P.G., 1994. Thermochronologic constraints on post-Paleozoic tectonic evolution of the central Transantarctic Mountains, Antarctica, *Tectonics,* **13,** 818–836.

Fitzgerald, P.G., Sandford, M., Barrett, P.J. & Gleadow, A.J., 1986. Asymmetric extension associated with uplift and subsidence in the Transantarctic Mountains and Ross Embayment, *Earth planet. Sci. Lett.,* **81,** 67–78.

Fouch, M.J., Fischer, K.M., Parmentier, E.M., Wysession, M.E. & Clarke, T.J., 2000. Shear wave splitting, continental keels, and patterns of mantle flow, *J. geophys. Res.,* **105,** 6255–6275.

Fretwell, P. *et al.*, 2013. Bedmap2: improved ice bed, surface and thickness datasets for Antarctica, *Cryosphere,* **7**(1), 375–393.

Gaherty, J.B., 2001. Seismic evidence for hotspot-induced buoyant flow beneath the reykjanes ridge, *Science,* **293**(5535), 1645–1647.

Gao, S., Davis, P.M., Slack, P.D., Rigor, A.W., Zorin, Y.A., Mordvinova, V.V., Kozhevnikov, V.M. & Logatchev, N.A., 1997. SKS splitting beneath continental rift zones, *J. geophys. Res.,* **102,** 22 781–22 797.

Garnero, E.J., Maupin, V., Lay, T. & Fouch, M.J., 2004. Variable azimuthal anisotropy in Earth's lowermost mantle, *Science,* **306**(5694), 259–261.

Goldstrand, P.M., Fitzgerald, P.G., Redfield, T.F., Stump, E. & Hobbs, C., 1994. Stratigraphic evidence for the Ross Orogeny in the Ellsworth Mountains, West Antarctica: implication for the evolution of the paleo-Pacific margin of Gondwana, *Geology,* **22,** 427–430

Granot, R., Cande, S.C., Stock, J.M., Davey, F.J. & Clayton, R.W., 2010. Postspreading rifting in the Adare Basin, Antarctica: regional tec- tonic consequences, *Geochem. Geophys. Geosyst.,* **11,** Q08005, doi:10.1029/2010GC003105.

Granot, R., Cande, S.C., Stock, J.M. & Damaske, D., 2013. Revised Eocene-Oligocene kinematics for the West Antarctic rift system, *Geophys. Res. Lett.,* **40,** 279–284.

Grindley, G.W. & Oliver, P.J., 1983. Palaeomagnetism of Cretaceous volcanic rocks from Marie Byrd Land, Antarctica, in *Antarctic Earth Science,* pp. 573–578, eds Oliver, R.L. *et al.*, Aust. Acad. Sci.

Grunow, A.M., Dalziel, I.W.D. & Kent, D.V., 1987. Ellsworth-Whitmore Mountains crustal block, western Antarctica: new paleomagnetic results and their tectonic significance, in *Gondwana Six: Structure, Tectonics and Geophysics,* Geophysical Monograph vol. 40, pp. 161–171, ed. McKenzie, G.D., American Geophysical Union.

Hamilton, R.J., Luyendyk, B.P., Sorlien, C.C. & Bartek, L.R., 2001. Cenozoic tectonics of the Cape Roberts rift basin and transantarctic mountains front, southwestern Ross Sea, Antarctica, *Tectonics,* **20**(3), 325–342.

Handler, M.R., Wysoczanski, R.J., Gamble, J.A., Horan, M.F., Brandon, A.D. & Neal, C.R., 2003. Proterozoic lithosphere in Marie Byrd Land, West Antarctica: Re-Os systematics of spinel peridotite xenoliths, *Chem. Geol.,* **196**(1–4), 131–145.

Henrys, S., Wilson, T., Whittaker, J.M., Fielding, C.R., Hall, J. & Naish, T.R., 2007. Tectonic history of mid-miocene to present southern victoria land basin, inferred from seismic stratigraphy in McMurdo Sound, Antarctica, Open-File Rep, U.S. *Geol. Surv.,* Short Research Paper 049.

Hernandez, S., Wiens, D., Anandakrishnan, S., Aster, R., Huerta, A., Nyblade, A. & Wilson, T., 2009. Seismic anisotropy of the Antarctic upper mantle from shear wave splitting analysis of POLENET and AGAP seismograms, *EOS, Trans. Am. geophys. Un.,* Fall Meet. Suppl.

Heeszel, D. *et al.*, , 2011. Seismic velocity structure of Antarctica from data collected during IPY, In *Proceedings of the 11th International Symposium on Antarctic Earth Sciences,* Edinburgh, Scotland, 10–16 July, 2011.

Hole, M.J. & LeMasurier, ,W.E., 1994. Tectonic controls on the geochemical composition of Cenozoic, mafic alkaline volcanic rocks from West Antarctica, *Contri. Mineral. Petrol.,* **117**(2), 187–202.

Huerta, A.D. & Harry, D.L., 2007. The transition from diffuse to focused extension: modeled evolution of the West Antarctic rift system, *Earth planet. Sci. Lett.,* **255,** 133–147.

Ingersoll, R.V., Cavazza, W., Baldridge, W.S. & Shafiqullah, M., 1990. Cenozoic sedimentation and paleotectonics of north-central New Mexico: implications for initiation and evolution of the Rio Grande Rift, *Geol. Soc. Am. Bull*., **102** (9),1280–1296.

Jordan, T.A., Ferraccioli, F., Vaughan, D.G., Holt, J.W., Corr, H., Blankenship, D.D. & Diehl, T.M., 2010. Aerogravity evidence for major crustal thinning under the Pine Island Glacier region (West Antarctica), *Geol. Soc. Am. Bull.,* **122**(5–6), 714–726.

Jordan, T.A. *et al.*, 2013. Inland Extent of the Weddell Sea Rift imaged by new aerogeophysical data, *Tectonophysics,* **585,** 137–160.

Jung, H. & Karato, S., 2001. Water-induced fabric transitions in olivine, *Science,* **293,** 1460–1463.

Katayama, I., Jung, H. & Karato, S., 2004. New type of olivine fabric from deformation experiments at modest water content and low stress, *Geology,* **32,** 1045–1048.

Karner, G.D., Studinger, M. & Bell, R.E., 2005. Gravity anomalies of sedimentary basins and their mechanical implications: Application to the Ross Sea basins, West Antarctica, *Earth planet. Sci. Lett.,* **235**(3–4), 577–596.

Keller, G.R., Khan, M.A., Morgan, P., Wendlandt, R.F., Baldridge, W.S., Olsen, K.H. & Braile, L.W., 1991. A comparative study of the Rio Grande and Kenya rifts, *Tectonophysics,* **197,** 355–371.

Karato, S., Jung, H., Katayama, I. & Skemer, P., 2008. Geodynamic significance of seismic anisotropy of the upper mantle: new insights from laboratory studies, *Annu. Rev. Earth planet. Sci.,* **36,** 59–95.

Kendall, J., Stuart, G.W., Ebinger, C.J., Bastow, I.D. & Keir, D., 2005. Magma-assisted rifting in Ethiopia, *Nature,* **433,** 146–148.

LeMasurier, W.E., 1990. Late Cenozoic volcanism on the Antarctic plate: an overview, *Antarctic Res. Ser.,* **48,** 1–17.

LeMasurier, W.E., 2008. Neogene extension and basin deepening in the west antarctic rift inferred from comparisons with the East African rift and other analogs, *Geology,* **36,** 247–250.

LeMasurier, W.E. & Rex, D.C., 1989. Evolution of linear volcanic ranges in Marie Byrd Land, West Antarctica, *J. geophys. Res.,* **94,** 7223–7236.

Lloyd, A. *et al.*, 2012. Reconciling geophysical and geochemical observations to understand craton lithosphere architecture, Abstract T23C-2695 presented at 2012 Fall Meeting, AGU, San Francisco, CA, 3–7 Dec.

Lloyd, A.J., Nyblade, A.A., Wiens, D.A., Hansen, S.E., Kanao, M., Shore, P.J. & Zhao, D., 2013. Upper mantle seismic structure beneath central East Antarctica from body wave tomography: implications for the origin of the Gamburtsev Subglacial Mountains, *Geochem. Geophys. Geosyst.,* **14,** 902–920.

Logatchev, N.A., Zorin, Y.A. & Rogozhina, V.A., 1983. Baikal Rift: active or passive? Comparison of the Baikal and Kenya rift zones, *Tectonophysics,* **94,** 223–240.

Long, M.D. & Becker, T.W., 2010. Mantle dynamics and seismic anisotropy, *Earth planet. Sci. Lett.,* **297,** 341–354.

Long, M.D. & Silver, P.G., 2009. Shear wave splitting and mantle anisotropy: measurements, interpretations, and new directions, *Surv. Geophys.,* **30,** 407–461.

Lough, A.C. *et al.*, 2013. Seismic detection of an active subglacial magmatic complex in Marie Byrd Land, Antarctica, *Nature Geosci.,* **6,** 1031–1035.

Luyendyk, B.P., 1995. Hypothesis for cretaceous rifting of east Gondwana caused by subducted slab capture, *Geology,* **23,** 373–376.

McKenzie, D., 1979. Finite deformation during fluid flow, *Geophys. J. R. astr. Soc.,* **58,** 689–715.

Mainprice, D., Tommasi, A., Couvy, H., Cordier, P. & Frost, D.J., 2005. Pressure sensitivity of olivine slip systems and seismic anisotropy of Earth's upper mantle, *Nature,* **433,** 731–733.

Miller, M.S. & Becker, T.W., 2012. Mantle flow deflected by interactions between subducted slabs and cratonic keels, *Nature Geosci.,* **5,** 726–730.

Miller, S.R., Fitzgerald, P.G. & Baldwin, S.L., 2001. Structure and kinematics of the central transantarctic mountains: constraints from structural geology and geomorphology near cape surprise, *Terra Antarc.,* **8**(1), 11–24.

Miller, M.S., Allam, A.A., Becker, T.W., Di Leo, J.F. & Wookey, J., 2013. Constraints on the tectonic evolution of the westernmost Mediterranean and northwestern Africa from shear wave splitting analysis, *Earth planet. Sci. Lett.,* **375,** 234–243.

Minster, J.B., Jordan, T.H., Molnar, P. & Haines, E., 1974. Numerical modelling of instantaneous plate tectonics-, *Geophys. J. R. astr. Soc.,* **36,** 541–576.

Mukasa, S.B. & Dalziel, I.W.D., 2000. Marie Byrd Land, West Antarctica: evolution of Gondwana's Pacific margin constrained by zircon U-Pb geochronology and feldspar common-Pb isotopic compositions, *Geol. Soc. Am. Bull.,* **112,** 611–627.

Müller, C., 2001. Upper mantle seismic anisotropy beneath Antarctica and the Scotia Sea region, *Geophys. J. Int.,* **147,** 105–122.

Nyblade, A. *et al.* 2012. A facility plan for polar seismic and geodetic science: meeting community needs through IRIS and UNAVCO polar services, Facility working plan and report for the National Science Foundation, Polar Networks Science Committee.

Obrebski, M., Castro, R.R., Valenzuela, R.W., van Benthem, S. & Rebollar, C.J., 2006. Shear-wave splitting observations at the regions of Northern Baja California and southern basin and range in Mexico, *Geophys. Res. Lett.,* **33**(5), doi:10.1029/2005GL024720.

Panning, M. & Romanowicz, B., 2006. A three-dimensional radially anisotropic model of shear velocity in the whole mantle, *Geophys. J. Int.,* **167,** 361–379.

Randall, D.E. & Mac Niocaill, C., 2004. Cambrian palaeomagnetic data confirm a natal embayment location for the Ellsworth-Whitmore mountains, Antarctica, in Gondwana reconstructions, *Geophys. J. Int.,* **157**(1), 105–116.

Reading, A.M. & Heintz, M., 2008. Seismic anisotropy of East Antarctica from shear-wave splitting: spatially varying contributions from lithospheric structural fabric and mantle flow? *Earth planet. Sci. Lett.,* **268,** 433–443.

Ritsema, J., Heijst, H.J. van & Woodhouse, J.H., 1999. Complex shear wave velocity structure imaged beneath Africa and Iceland, *Science,* **286,** 1925–1928.

Rocchi, S., Amienti, P., D'Orazio, M., Tonarini, S., Wijbrans, J.R. & Vincenzo, G.D., 2002. Cenozoic magmatism in the western Ross Embayment: role of mantle plume versus plate dynamics in the development of the West Antarctic rift system, *J. geophys. Res.,* **107,** ECV 5-1–ECV 5-22.

Rowell, A.J., Van Schmus, W.R., Storey, B.C., Fetter, A.H. & Evans, K.R., 2001. Latest neoproterozoic to mid-cambrian age for the main deformation phases of the transantarctic mountains: new stratigraphic and isotopic constraints from the Pensacola mountains, Antarctica, *J. geol. Soc. Lond.,* **158**(2), 295–308

Rümpker, G. & Silver, P.G., 2000. Calculating splitting parameters for plume-type anisotropic structures of the upper mantle, *Geophys. J. Int.,* **143,** 507–520

Savage, M.K., 1999. Seismic anisotropy and mantle deformation: what have we learned from shear wave splitting? *Rev. Geophys.,* **37,** 65–106.

Schilling, J.G., 1973a. Afar Mantle Plume: rare earth evidence, *Nature,* **242,** 2–5.

Schilling, J.G., 1973b. Iceland mantle plume: geochemical study of Reykjanes Ridge, *Nature,* **242,** 565–571.

Schopf, J.M., 1969. Ellsworth Mountains: position in West Antarctica due to sea-floor spreading, *Science,* **164**(3875), 63–66.

Siddoway, C.S., Baldwin, S.L., Fitzgerald, P.G., Fanning, C.M. & Luyendyk, B.P., 2004. Ross Sea mylonites and the timing of intracontinental extension within the West Antarctic rift system, *Geology,* **32,** 57–60.

Sieminski, A., Debayle, E. & Lévêque, J.J., 2003. Seismic evidence for deep low-velocity anomalies in the transition zone beneath West Antarctica, *Earth planet. Sci. Lett.,* **216,** 645–661.

Silver, P.G., 1996. Seismic anisotropy beneath the continents: probing the depths of geology, *Ann. Rev. Earth planet. Sci.,* **24,** 385–432.

Silver, P.G. & Chan, W.W., 1988. Implications for continental structure and evolution from seismic anisotropy, *Nature,* **335,** 34–39.

Silver, P.G. & Chan, W.W., 1991. Shear wave splitting and subcontinental mantle deformation, *J. geophys. Res.,* **96,** 16 429–16 454.

Stamps, D.S., Calais, E., Saria, E., Hartnady, C., Nocquet, J.-M., Ebinger, C.J. & Fernandes, R.M., 2008. A kinematic model for the East African Rift, *Geophys. Res. Lett.,* **35,** L05304, doi:10.1029/2007GL032781.

Storey, B.C. & Dalziel, I.W.D., 1987. Outline of the structural and tectonic history of the Ellsworth Mountains-Thiel Mountains Ridge, West Antarctica, in *Gondwana Six: Structure, Tectonics, and Geophysics,* pp. 117–128, ed. McKenzie, G.D., American Geophysical Union, Geophysical Monograph Number 40.

Storey, B.C., 1995. The role of mantle plumes in continental breakup: case histories from gondwanaland, *Nature,* **377**(6547), 301–308.

Storey, B.C., Leat, P.T., Weaver, S.D., Pankhurst, R.J., Bradshaw, J.D. & Kelley, S., 1999. Mantle plumes and Antarctica-New Zealand rifting: evidence from mid-cretaceous mafic dykes, *J. geol. Soc. Lond.,* **156,** 659–671.

Stump, E., 1995. *The Ross Orogen of the Transantarctic Mountains,* Cambridge Univ. Press.

Stump, E. & Fitzgerald, P.G., 1992. Episodic uplift of the Transantarctic Mountains, *Geology,* **20,** 161–164.

Teanby, N.A., Kendall, J.M. & Van Der Baan, M., 2004. Automation of shear-wave splitting measurements using cluster analysis, *Bull. seism. Soc. Am.,* **94,** 453–463.

Ten Brink, U.T., Hackeny, R.I., Bannister, S., Stern, T.A. & Makowsky, Y., 1997. Uplift of the Transantarctic Mountains and the bedrock beneath the East Antarctic ice sheet, *J. geophys. Res.,* **102,** 27 603–27 622.

Thybo, H. & Nielsen, C., 2009, Magma-compensated crustal thinning in continental rift zones, *Nature,* **457,** 873–876.

Trey, H., Cooper, A.K., Pellis, G., della Vedova, B., Cochrane, G., Brancolini, G. & Makris, J., 1999. Transect across the West Antarctic rift system in the Ross Sea, Antarctica, *Tectonophysics,* **301,** 61–74.

Usui, Y., Kanao, M., Kubo, A., Hiramatsu, Y. & Negishi, H., 2007. Upper mantle anisotropy from teleseismic SKS splitting beneath Lützow-Holm Bay region, East Antarctica: a keystone in a changing world-online proceedings of the 10th ISAES, eds Cooper, A.K. *et al.*, Open-File Rep, U.S. Geol. Surv. 2007–1047, Short Research Paper 013, 4 p.

Vauchez, A., Tommasi, A., Barruol, G. & Maumus, J., 2000. Upper mantle deformation and seismic anisotropy in continental rifts, *Phys. Chem. Earth,* **25,** 111–117.

Vinnik, L.P., Makeyeva, L.I., Milev, A. & Usenko, A.Y., 1992. Global patterns of azimuthal anisotropy and deformations in the continental mantle, *Geophys. J. Int.,* **111,** 433–447.

Walker, K.T., Nyblade, A.A., Klemperer, S.L., Bokelmann, G.H.R. & Owens, T.J., 2004. On the relationship between extension and anisotropy: constraints from shear wave splitting across the East African plateau, *J. geophys. Res.,* **109,** 1–21.

Walker, K.T., Bokelmann, G.H. R., Klemperer, S.L. & Bock, G., 2005. Shear-wave splitting around the Eifel hotspot: evidence for a mantle upwelling, *Geophys. J. Int.,* **163,** 962–980.

Wang, X., Ni, J., Aster, R., Sandvol, E., Wilson, D., Sine, C., Grand, S. & Baldridge, W.S., 2008. Shear wave splitting and mantle flow beneath the Colorado Plateau and its boundary with the Great Basin, *Bull. seism. Soc. Am.,* **98,** 2526–2532.

Watts, D.R. & Bramall, A.M., 1981. Paleomagnetic evidence for a displaced terrain in western Antarctica, *Nature,* **293**(5834), 638–641.

Weaver, S.D., Storey, B.C., Pankhurst, R.J., Mukasa, S.B., DiVenere, V.J. & Bradshaw, J.D., 1994. Antarctica-New Zealand rifting and Marie Byrd Land lithospheric magmatism linked to ridge subduction and mantle plume activity, *Geology,* **22,** 811–814.

Wilson, T.J., 1995. Cenozoic transtension along the Transantarctic Mountains-West Antarctic rift boundary, southern Victoria Land, Antarctica, *Tectonics,* **14,** 531–545.

Wilson, D.S. & Luyendyk, B.P., 2006. Bedrock platforms within the ross embayment, west antarctica: hypotheses for ice sheet history, wave

erosion, cenozoic extension, and thermal subsidence, *Geochem. Geophys. Geosyst.,* **7**(12), doi:10.1029/2006GC001294.

Wilson, T. & The POLENET Group, 2011. The Antarctic-POLENET (ANET) GPS Network in West Antarctica, In *Proceedings of the 11th International Symposium on Antarctic Earth Sciences,* Edinburgh, 10–16 July, 189. Available at: http://www.isaes2011.org.uk/abstracts_v4_20_07_2011.pdf (last accessed 2 March 2014).

Winberry, J.P. & Anandakrishnan, S., 2004. Crustal structure of the West Antarctic rift system and Marie Byrd Land hotspot, *Geology,* **32,** 977–980.

Wolfe, C.J. & Silver, P.G., 1998. Seismic anisotropy of oceanic upper mantle: shear wave splitting methodologies and observations, *J. geophys. Res.,* **103,** 749–771

Wolfe, C.J. & Solomon, S.C., 1998. Shear-wave splitting and implications for mantle flow beneath the MELT region of the East Pacific Rise, *Science,* **280,** 1230–1232.

Wüstefeld, A. & Bokelmann, G., 2007. Null detection in shear-wave splitting measurements, *Bull. seism. Soc. Am.,* **97,** 1204–1211,

Xue, M. & Allen, R., 2005. Asthenospheric channeling of the Icelandic upwelling: evidence from seismic anisotropy, *Earth planet. Sci. Lett.,* **235,** 167–182.

Xue, M. & Allen, R.M., 2006. Origin of the newberry hotspot track; evidence from shear-wave splitting, *Earth planet. Sci. Lett.,* **244,** 315–322.

Zhang, S. & Karato, S., 1995. Lattice preferred orientation of olivine aggregates deformed in simple shear, *Nature,* **375,** 774–777.

SUPPORTING INFORMATION

Additional Supporting Information may be found in the online version of this article:

Figure S1. Individual A and B quality splitting results for all events stacked in the final solutions for all stations used in this study.
Table S1. A summary of individual splitting results for all events stacked in the final solutions for all stations used in this study. Parameters listed include the station of interest, the event time, the core-phase used, the SNR for the radial (R-SNR), transverse (T-SNR), and vertical (Z-SNR) components, the back-azimuth for the event-station pair (BAZ), the polarization azimuth (PAZ), the orientation of the fast axis, the magnitude of the delay time (Lag), and the graded quality of the measurement (Grade).
(http://gji.oxfordjournals.org/lookup/suppl/doi:10.1093/gji/ggu117/-/ DC1).

Please note: Oxford University Press is not responsible for the content or functionality of any supporting materials supplied by the authors. Any queries (other than missing material) should be directed to the corresponding author for the article.